© Technion - Israel Institute of Technology, Elyachar Central Library

הטכניון – מכון טכנולוגי לישראל
Technion – Israel Institute of Technology

ספריות הטכניון
The Technion Libraries

בית הספר ללימודי מוסמכים ע"ש ארווין וג'ואן ג'ייקובס
Irwin and Joan Jacobs Graduate School

©
All rights reserved

This work, in whole or in part, may not be copied (in any media), printed, translated, stored in a retrieval system, transmitted via the internet or other electronic means, except for "fair use" of brief quotations for academic instruction, criticism, or research purposes only.
Commercial use of this material is completely prohibited.

©
כל הזכויות שמורות

אין להעתיק (במדיה כלשהי), להדפיס, לתרגם, לאחסן במאגר מידע, להפיץ באינטרנט, חיבור זה או כל חלק ממנו, למעט "שימוש הוגן" בקטעים קצרים מן החיבור למטרות לימוד, הוראה, ביקורת או מחקר. שימוש מסחרי בחומר הכלול בחיבור זה אסור בהחלט.

© Technion - Israel Institute of Technology, Elyachar Central Library

Microstructure and Properties of TiCN CVD Coatings

Gadi Greenman

© Technion - Israel Institute of Technology, Elyachar Central Library

Microstructure and Properties of TiCN CVD Coatings

RESEARCH THESIS

SUBMITTED AS PARTIAL FULFILLMENT OF THE REQUIREMENTS FOR THE DEGREE OF MASTER OF SCIENCE IN MATERIALS ENGINEERING

GADI GREENMAN

Submitted to Senate of the
Technion – Israel Institute of Technology

Ayar 5771 Haifa May 2011

© Technion - Israel Institute of Technology, Elyachar Central Library

Acknowledgements

I would like to thank my supervisor Prof. Wayne D. Kaplan for his invaluable professional advice and support. I would also like to thank Dr. Alex Berner, of the Materials Engineering Department at the Technion, for his support in SEM-EBSD analysis. Many thanks to my colleagues at ISCAR, Ms. Mariana Leiderman for XRD analysis, and Mr. Sagiv Kalai for nanoindentation tests and general assistance.

Lastly, I offer my regards and blessings to my family who supported me in every respect throughout the course of this degree.

© Technion - Israel Institute of Technology, Elyachar Central Library

TABLE OF CONTENTS

ABSTRACT **9**

LIST OF SYMBOLS AND ACRONYMS **10**

1 INTRODUCTION **11**

2 LITERATURE SURVEY **12**

2.1 Hardmetal Cutting Tools Used in Turning Applications **12**

2.2 Cemented Carbide Substrates Based on WC-Co **15**

2.3 Chemical Vapor Deposition (CVD) Coatings **16**

2.3.1 CVD Technique 17

2.3.1.1 Titanium Nitride (TiN) 20

2.3.1.2 Moderate Temperature Titanium Carbon Nitride (MT-TiCN) 21

2.3.1.3 Thermal cracks due to residual stress 23

2.4 Importance of coating thermal stability in wear processes **24**

2.5 Tribological Properties **25**

2.5.1 Cutting tests 26

2.6 Research goals **29**

3 EXPERIMENTAL METHODS AND PROCEDURES **30**

3.1 Coatings experiments **30**

3.1.1 Design of Experiments 30

3.1.2 Sample preparation 32

3.1.3 Loading method 32

3.1.4 Deposition process 33

3.2 Optical investigation **34**

3.2.1 Coating Thickness Measurement 34

3.2.2 Thermal cracks 34

© Technion - Israel Institute of Technology, Elyachar Central Library

3.3 Evaluation of the Microstructure 34
3.3.1 Scanning Electron Microscopy (SEM) Investigation 34
3.3.2 X-ray Diffraction Analysis (XRD) 35
3.3.3 Texture analysis by SEM-EBSD 36
3.3.4 Stylus instrument for Surface Roughness Measurements 37
3.4 Evaluation of Mechanical Properties 37
3.4.1 Nano-hardness measurements 37
3.4.2 Evaluation of the adhesion 38
3.5 Thermal stability 39
3.5.1 Measurement of resistance to oxidation 39
3.6 Tribological properties 39
3.6.1 Interrupted cutting test on AISI 1060 39
3.6.2 Continuous cutting test on AISI 1045 40
4 RESULTS 42
4.1 Evaluation of the Microstructure 42
4.1.1 Scanning Electron Microscopy (SEM) Results 42
4.1.2 SEM-EBSD Results 43
4.1.3 X-ray Diffraction Analysis (XRD) 44
4.2 Optical Microscopy 49
4.2.1 Coating Thickness 49
4.2.2 Thermal cracks 49
4.3 Evaluation of Mechanical Properties 51
4.3.1 Surface Roughness 51
4.3.2 Hardness measurements 52
4.3.3 Evaluation of the adhesion 53
4.4 Thermal oxidation 54
4.5 Tribological properties 55
4.5.1 Interrupted cutting test on SAE1060 55
4.5.2 Continuous cutting test on AISI 1045 56

5 DISCUSSION 59

5.1 Influence of deposition parameters on MT-TiCN microstructure 59

5.2 Influence of MT-TiCN microstructure on mechanical properties 60

5.2.1 Surface Roughness dependence on microstructure 60

5.2.2 Hardness dependence on microstructure 61

5.2.3 Oxidation resistance 62

5.3 Cutting tests 62

5.3.1 Interrupted cutting test 62

5.3.2 Continuous cutting test results dependence mechanical properties 64

6 SUMMARY AND CONCLUSIONS 65

7 RECOMMENDATION FOR FUTURE WORK 66

8 REFERENCES 67

© Technion - Israel Institute of Technology, Elyachar Central Library

© Technion - Israel Institute of Technology, Elyachar Central Library

LIST OF FIGURES

Figure 1: Cutting tool with its main components 13
Figure 2: Cutting tool insert for turning applications 14
Figure 3: Hard coatings for cutting tools application 16
Figure 4: CVD coating unit for deposition Ti(C, N) coatings 17
Figure 5: CVD coating system for indexable inserts. 18
Figure 6: Coated Indexable insert. (a) indexable coated insert; and 19
Figure 7: Deposition of TiN on a carbide substrate 21
Figure 8: Schematic drawing of MT-TiCN deposition on a TiN layer 22
Figure 9: Schematic representation of various types of failure 24
Figure 10: Classification of insert 27
Figure 11: Schematic presentation of deposition parameter range used in this study. 31
Figure 12: Machine for inserts preparation before coating. 32
Figure 13: Inserts loading method for uniform thickness distribution. 32
Figure 14: Schematic presentation of the deposition process 33
Figure 15: Oxidation layer (TiO_2) thickness measurement by SEM. 39
Figure 16: Photographs of the raw material (AISI 1060) used for interrupted tests. 40
Figure 17: Photographs of the raw material (AISI 1045) used for continuous tests. 41
Figure 18: SEM micrographs of the coating microstructure 42
Figure 19: Five fold grains identification by SEM-EBSD analysis. 43
Figure 20: Specified crystallographic direction of selected five fold structure 44
Figure 21: Pareto plot for (220) oriented grains. 46
Figure 22: Factorial model for (220) oriented grains. 46
Figure 23: Pareto plot for (311) oriented grains. 47
Figure 24: Factorial model for (311) oriented grains. 47
Figure 25: Pareto plot for (422) oriented grains. 48
Figure 26: Factorial model for (422) oriented grains. 48
Figure 27: Plan view of polished samples for thermal crack investigations. 50
Figure 28: Pareto plot for roughness results. 51
Figure 29: Factorial model roughness results. 52
Figure 30: Pareto plot for hardness results. 53
Figure 31: Factorial model for hardness results. 53
Figure 32: Pareto plot for oxidation rate measurements. 54
Figure 33: Factorial model of oxidation rate measurements. 55
Figure 34: Typical failure during interrupted conditions 56
Figure 35: Interrupted cutting test results. 56
Figure 36: Progress of wear during continuous cutting test. 57
Figure 37: Continuous cutting test results. 58
Figure 38: SEM micrograph of the coarse microstructure nucleation 59
Figure 39: Spiral growth mechanism 61
Figure 40: SEM plan view image of the high temperature coating. 61
Figure 41: Schematic presentation of cracks penetration depth. 63

© Technion - Israel Institute of Technology, Elyachar Central Library

LIST OF TABLES

Table 1: Schedule for trial deposition conditions. 31
Table 2: Preferred orientation of the CVD experimental coatings. 44
Table 3: Coating thickness results of selected experiments. 49
Table 4: Surface roughness of trial coatings. 51
Table 5: Hardness results of the coatings 52
Table 6: Oxidation rate measurements of trial coatings. 54

© Technion - Israel Institute of Technology, Elyachar Central Library

ABSTRACT

Medium temperature chemical vapor deposition (MTCVD) coatings on cemented carbide cutting tools have gained prominence in the machining of gray and nodular cast iron, steels, and other abrasive materials, that require increased edge toughness and wear resistance of the cutting tools. MTCVD TiCN is the most common coating layer used for conventional cutting tools.

TiCN coatings produced by MTCVD were investigated. The influence of CVD deposition variables such as temperature, pressure and H_2 flow on the preferred orientation, grain size, surface morphology, deposition rate, surface roughness, hardness and thermal stability was investigated. The preferred orientation of the TiCN MT was characterized using X-ray diffraction (XRD). Scanning electron microscopy (SEM) and optical microscopy was used to characterize the morphology of the coating.

The deposited TiCN MT coatings had a twinned columnar microstructure with a preferred orientation that depends on deposition conditions. The results indicated that the deposition temperature is a critical factor that can be effectively used to control the morphology and structure of the coating. High temperature deposition results in the formation of a {220} preferred orientation. Low temperature deposition conditions results in {311} and {422} preferred orientation.

Control of the microstructure provides a method to optimize the mechanical properties for a specific cutting application. For example, TiCN MT coatings deposited at 750^{o}C tend to be more stable during interrupted cutting conditions because of low hardness. On the other hand, higher temperature deposition (975^{o}C) resulted in improved results for continuous cutting because of high hardness and thermal stability.

© Technion - Israel Institute of Technology, Elyachar Central Library

LIST OF SYMBOLS AND ACRONYMS

CVD	Chemical Vapor Deposition
PVD	Physical Vapor Deposition
Vc	cutting speed
f	feed
A	depth of cut
D	diameter of the workpiece
n	rotational velocity
Ea	activation energy of the reaction
k	Boltzmann constant
T	deposition temperature
P	deposition pressure
SEM	Scanning Electron Microscopy
XRD	X-ray Diffraction
EBSD	Electron Backscatter Diffraction
Ra	average surface roughness

© Technion - Israel Institute of Technology, Elyachar Central Library

1 INTRODUCTION

Chemical vapor deposition (CVD) is a widely used technology. The majority of its application involves applying solid thin-film coatings to the surface. CVD involves flowing a precursor gas or gases into a chamber containing one or more heated objects to be coated. Chemical reactions occur on and near the hot surface, resulting in the deposition of a thin film on the surface. This is accompanied by the production of chemical by-products that are exhausted out of the chamber along with unreacted precursor gases.

CVD has a number of advantages as a method for depositing thin films. One of the primary advantages is that the thickness on the sidewalls of parts is comparable to the thickness on the top. This means that films can be applied to elaborately shaped pieces, including the insides and undersides of the coated part, and that high-aspect ratio holes and other features can be completely coated.

CVD also has a number of disadvantages. One of the primary disadvantages lies in the properties of the gases. CVD precursors can be highly toxic, explosive or corrosive. The byproducts of CVD reactions can also be hazardous. Some of these precursors, especially the metal-organic precursors, can also be quite costly. The other major disadvantage is the fact that the films are usually deposited at elevated temperatures. This puts some restriction on the kind of substrates that can be coated. More importantly, it leads to stresses in films deposited on materials with different thermal expansion coefficients, which can cause mechanical instabilities in the deposited film.

The choice of CVD precursors is determined by many factors in addition to the requirement that it contains the elements of interest. These considerations include the decomposition temperature required, vapor pressure of the precursor species, cost and safety.

© Technion - Israel Institute of Technology, Elyachar Central Library

2 LITERATURE SURVEY

The current chapter contains background information on coated cutting tool inserts used in turning. It starts with describing cutting tool inserts, basic requirements from cutting tool material and the application of turning. Then, substrates based on WC-Co are introduced, as well as the coating technique of CVD (Chemical Vapor Deposition). The coatings encountered in this research are described, i.e. TiN and MT TiCN.

2.1 Hardmetal Cutting Tools Used in Turning Applications

In our everyday life many tools and equipment we use are machined from steel. To obtain the required shapes and forms, a cutting tool material is needed which is harder than steel, such as hardmetals. The most important properties for cutting tool inserts are a low friction coefficient, oxidation resistance, chemical stability, hot hardness, abrasive wear resistance, crack resistance and good thermal properties.

The present research deals with hardmetal cutting tool inserts consisting of a substrate and a coating. The substrate is based on WC-Co, which is milled, pressed and then sintered at about 1350 to 1450^{o}C. The properties of coated hardmetal cutting tool inserts vary with their application.

This investigation focused on cutting tool inserts of the main machining group P (according to ISO 513), cutting tools for cutting of steels. The hardmetal grades of this group contain WC, TiC, TaC and NbC in the form of mixed crystals with Co. They are distinguished by their excellent high-temperature strength and low abrasion and are used for the turning of steel (ferrous metal).

© Technion - Israel Institute of Technology, Elyachar Central Library

A cutting tool with its main components is displayed in Figure 1.

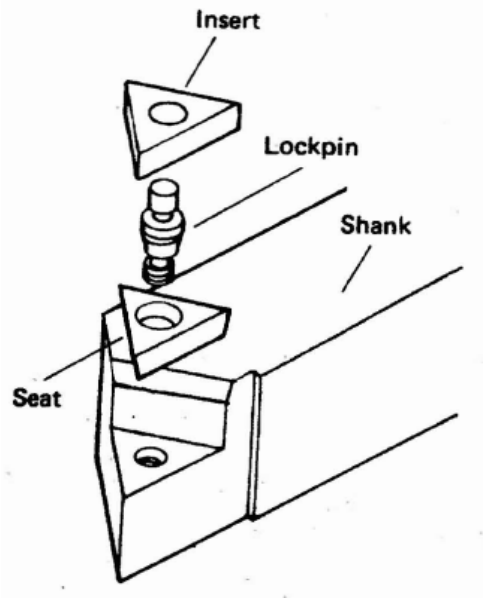

Figure 1: Cutting tool with its main components [1].

Cutting tool inserts cut metal because they are sharp and harder than the workpiece. The insert is attached with the lockpin to the seat and then it is fixed with the same pin to the shank or holder. When all cutting edges have been worn, the insert is discarded.

Basic requirements placed on the cutting tool material include [2]:

- high hardness against abrasion at the points of contact with raw material;
- high temperature hardness and compressive strength against plastic deformation of the cutting edge during cutting process;
- high thermal stability and high temperature wear resistance against diffusion wear;
- good internal bond strength against adhesive wear shearing of pressure welded material;
- good toughness and edge strength against cutting edge fracture through external forces;
- small difference between thermal coefficient of expansion values of the individual structural components, in order to avoid formation of cracks.

© Technion - Israel Institute of Technology, Elyachar Central Library

In order to answer to these entire requirements the combination of a substrate and suitable coating is essential.

The cutting tool inserts investigated are all used for turning. This operation generates cylindrical shapes with a single touch point where the tool is stationary and the workpiece rotates (Figure 2b).

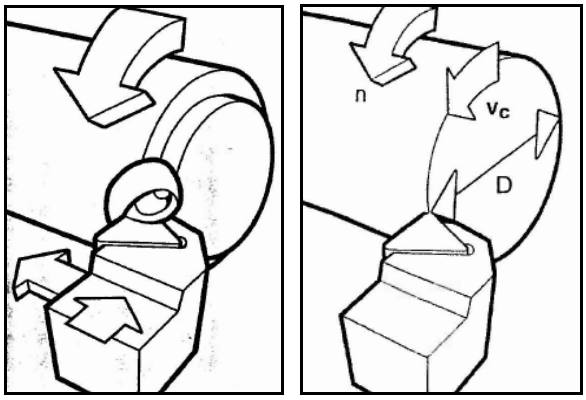

(a) (b)

Figure 2: Cutting tool insert for turning applications [3]. (a) definition of the cutting speed; (b) chip formation.

Turning involves two movements, the rotation of the workpiece and the feed of the tool. The cutting speed (Vc) or surface speed in m/min is described as:

$$Vc = D \times \pi \times n / 1000 \text{ [m/min]} \qquad (1)$$

where: D is the diameter of the workpiece in mm, and n is a rotational velocity in rpm.

In Figure 2b, the metal turning process has already started, as a formed chip can be identified. In metal cutting, the cut material generates chips which flow over the rake face (top side) of the insert and the shape and size depend on the geometry of the cutting insert.

© Technion - Israel Institute of Technology, Elyachar Central Library

2.2 Cemented Carbide Substrates Based on WC-Co

These substrates consist of carbides cemented by a Co-rich binder phase. To improve the wear resistance of a pure WC-Co substrate, other elements are often added, such as cubic transitional metal carbides like TiC, TaC, NbC. The main purpose of the substrate is to support the coating and to provide crack arrest to prevent failure, if and when mechanical or thermal cracks penetrate the coating [21]

Exner [4] described cemented carbides as single crystals of one or more carbide phases which form a continuous skeleton where the free space is filled by a metal binder (Co). The microstructure of cemented carbide influences its properties, the most important features being the mean grain size of the carbide crystals, the mean free path in the binder phase and the contiguity of the carbide skeleton.

The binder phase fills the spaces within the carbide skeleton during the liquid phase sintering process and forms interfaces between the binder phase and the carbide phases. The size of grains influence mechanical properties, usually the finer the sintered grains, the higher the hardness, and the lower the toughness and transverse rupture strength [5]. Schaller [6] investigated the mechanical behavior of WC with 11 wt.% Co by bending tests, internal friction and electron microscopy. During the cutting process, high temperatures develop which affect the behavior of hardmetals. Tests resulted in the definition of three temperature ranges according to their mechanical behavior. From room temperature up to 650^{o}C, the material was elastic and brittle. Between 650 and 850^{o}C, a limited local plasticity was observed due to the strong hardening during deformation. Above 850^{o}C, the cemented carbide deformed and behaved according to creep curves.

A cemented carbide cutting insert, for turning applications, based on WC-Co, is often coated by CVD to increase its tool life. The coating process takes place at high temperatures, and during the cooling process cracks are often formed in the surface layers. Those cracks are of course undesirable as they can propagate during the cutting of the workpiece. To stop propagating cracks, graded substrates are used with increased toughness which in turn increases the resistance to crack propagation.

© Technion - Israel Institute of Technology, Elyachar Central Library

2.3 Chemical Vapor Deposition (CVD) Coatings

The coating of hardmetal inserts with a hard material layer has enabled, for machining of steels, the cutting time to be extended and thus tooling costs to be reduced. Alternatively, the cutting speed may be increased which results in higher rate of productivity. By coating with a hard material, the combination of an extremely wear resistant surface layer with a tough, mechanically shock resistant base material can be achieved. Two basic methods are presently available to hard coat base materials, namely CVD and physical vapor deposition (PVD). The CVD process will now be discussed.

It is possible using CVD to obtain coatings of metals, oxides, nitrides, carbides and borides with strong bonding to a substrate (see Figure 3). The hard coatings listed in Figure 3 have proven particularly suitable for cutting tool applications.

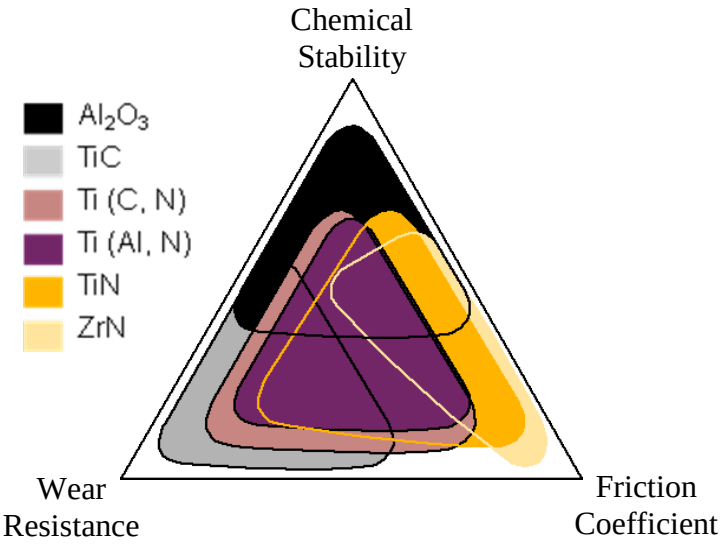

Figure 3: Hard coatings for cutting tools application.

Each coating has a unique characteristic property. For example, alumina (Al_2O_3) is a chemical stable coating that can protect substrates from high temperatures during machining. Ti(C,N) coatings shows good wear resistance, important for turning applications.

© Technion - Israel Institute of Technology, Elyachar Central Library

As was mentioned before, the cutting insert should be coated for mechanical property improvement. Desirable coatings can be deposited onto standard cemented carbide tool inserts using a CVD coating system. Precursors in use and deposition temperatures depend on the coating type. The deposition temperature is usually in the range of 800 to 1015^{o}C. A schematic layout of a CVD coating unit is shown in Figure 4.

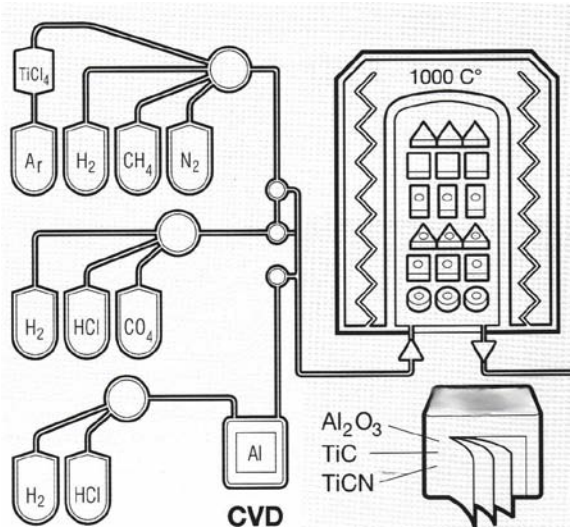

Figure 4: CVD coating unit for deposition Ti(C, N) coatings [3].

2.3.1 CVD Technique

Thermodynamic calculations of CVD processes based on minimization of the Gibbs free energy of the gas-solid system are useful to predict the influence of process variables such as temperature, pressure, inlet gas concentration on the phase structure. The thermodynamic equilibrium calculations can only indicate a tendency with respect to the rate of reaction and there by rate of growth. A more exact statement of the rate of deposition is problematic since it is extremely difficult to comprehend the mechanism of flow.

© Technion - Israel Institute of Technology, Elyachar Central Library

The deposition process can be divided in to the following steps:

- Transport of the reactants to the substrate;
- Absorption of the reactants onto the substrate;
- Nucleation and start of the reaction, under the prevailing conditions and participation of the substrate;
- Removal of the reaction products.

The following parameters are generally available for undertaking the CVD process:

- Temperature;
- Pressure;
- Gas composition;
- Chemical activity of the substrate;
- Gas throughput (speed of flow).

Figure 5 illustrates a modern CVD coating system.

(a) (b)

Figure 5: CVD coating system for inserts. (a) gas cabinet; (b) reactor and furnace.

The gas cabinet (Figure 5a) includes mass flow controllers (MFC) for accurate gas supply. The coating reactor (Figure 5b) must be constructed so as to resist a temperature of 1100^{o}C because of a required coating temperature of around 1000^{o}C. The coating reactor is produced from a high temperature nickel alloy.

The furnace dimension of the reactor should be such that an exact predetermined temperature profile can be achieved. It is usual to use a vertical reactor, bell type, furnace

© Technion - Israel Institute of Technology, Elyachar Central Library

(Figure 5b). The deposition of a uniform coating thickness throughout the vessel is a major pre-requirement for a CVD unit. The dosing of the correct amount of gas is carried out using calibrated mechanical and electronic flow meters.

The gas enriched with HCl, which is produced by the coating process, must be neutralized. It is an advantage, in equipment which operates in a coarse vacuum of 60 to 700 mbar, to carry out the neutralization in the pump medium (NaOH) of a liquid ring pump.

CVD coatings of the cemented carbide cutting tools with TiC and TiN were developed by the beginning of the 1950s. Modern coated cutting inserts consist of at least two types of coatings. A thick, hard coating can assist a softer substrate in carrying the load and thus decrease the contact area and the friction [24].

The cutting speed and thus productivity of the chip producing technique (machining) can be increased by using a combination of different coatings (Figure 6).

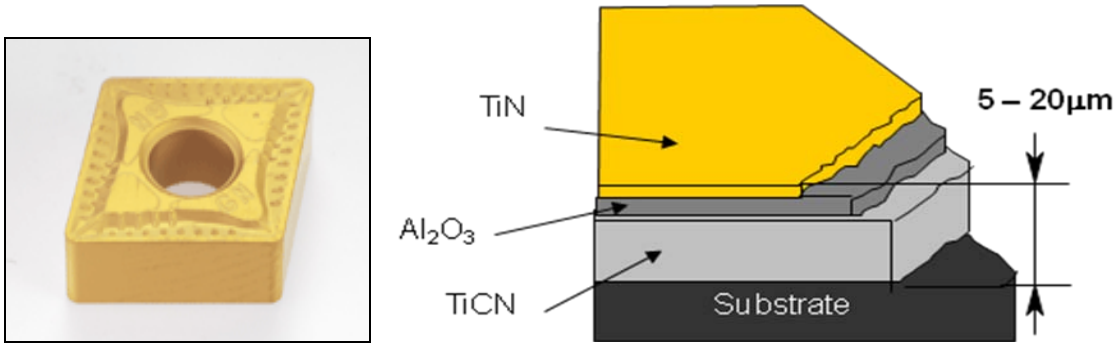

(a) (b)

Figure 6: (a) Coated insert; and (b) schematic cross section of the insert.

The cutting forces are generally reduced by 10 to 15% and the cutting temperature is markedly lower than in the case of uncoated inserts. This is due to the favorable level of friction. The following are predominantly used as a coating material for cutting tools applications: titanium carbide (TiC); titanium nitride (TiN); titanium carbo-nitride

© Technion - Israel Institute of Technology, Elyachar Central Library

(TiCN); and aluminium oxide (alumina – Al_2O_3). CVD processes for titanium nitride (TiN) and moderate temperature titanium carbon nitride (MT-TiCN) will now described in detail.

2.3.1.1 Titanium Nitride (TiN)

The nitrides of the group metals, such as Ti, Zr, Hf, show high hardness, low friction coefficient and good wear resistance. Therefore, they are used in cutting tools and wear-resistant components. TiN, for example is used as single coating on conventional hardmetals to increase cutting performance [11].

Titanium Nitride (TiN) is used extensively as a CVD coating mainly for wear and erosion resistance. TiN has a cubic structure (FCC) with a melting point of 2950^{o}C. When deposited from a $TiCl_4$, N_2, H_2 system the formation of TiN can be described by:

$$TiCl_4 + 1/2N_2 + 2H_2 = TiN + 4HCl \qquad (2)$$

A mixture of titanium tetra-chloride ($TiCl_4$), nitrogen (N_2) and hydrogen (H_2) is produced in a gas mixing unit, which is then led into a reactor chamber over the parts to be coated (Figure 7). The reaction takes place at about 800 to 900^{o}C and at wide range of pressure, between 300-900 mbar. TiN is usually used as an intermediate layer between the WC-Co substrate and the TiCN coatings. In multi layered system, TiN is essential for adhesion (coating to substrate) improvement and serves as a diffusion barrier against substrate elements into the coating [21,40].

© Technion - Israel Institute of Technology, Elyachar Central Library

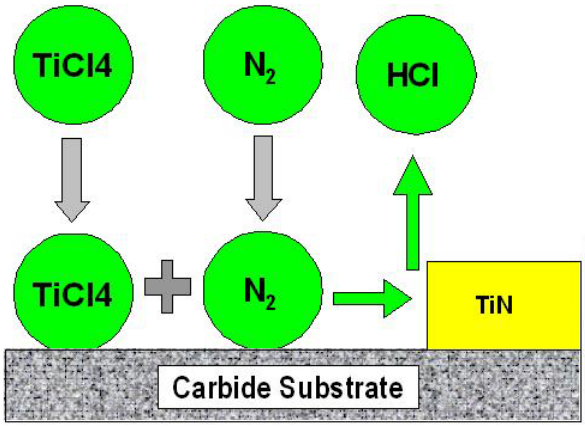

Figure 7: Deposition of TiN on a carbide substrate.

TiN is economical and has been extensively studied. Shaviv [7] reported the optimum reaction parameters of TiN, such as reaction temperature, pressure and morphology substrate. The effect on adhesion of TiN coatings to cemented carbides was reported by Laugier [11]. Scratch and indentation tests were used to investigate coating failure at temperatures of cutting tool applications (~ 850^{o}C). WC-Co substrates were coated with TiN using CVD at 1000^{o}C with a thickness of 6 µm. The adhesion test by indentation was applied. It was found that adhesion quality of TiN layer is better in high temperature deposition due to significant substrate softening [11].

2.3.1.2 Moderate Temperature Titanium Carbon Nitride (MT-TiCN)

There are two types of TiCN deposition processes, which are distinguished by different temperatures. So-called high temperature (HT) TiCN coatings are deposited from $TiCl_4$, CH_4 and N_2 at a temperature of ~1000^{o}C while the so-called moderate temperature (MT) TiCN is deposited at ~ 850 - 950^{o}C. The latter process is today more popular [18,21].

The lower temperature reduces decarburization of the cemented carbide substrate during the coating process, and reduces the amount of brittle η-carbides, which improves mechanical properties of a cutting tool [21,29]. High temperature coatings, TiC or TiCN coated inserts, can develop an unwanted brittle η phase at the interface [30]. Reducing process temperature below 850^{o}C can lead to additional improvement in cutting tool life.

© Technion - Israel Institute of Technology, Elyachar Central Library

The aspect of process temperature influence on mechanical properties should be investigated.

A mixture of titanium tetra-chloride ($TiCl_4$), azetonetril (CH_3CN) and hydrogen (H_2) is produced in a gas mixing unit, which is then led into a reactor chamber over the parts to be coated (Figure 8). The chamber is heated to a required temperature. Under specific conditions of temperature, pressure and gas composition a layer of MT-TiCN is deposited on the insert surface. Equation (3) applies to the formation of moderate temperature titanium carbide nitride (MT-TiCN) from the $TiCl_4$, CH_3CN, H_2 system.

$$4TiCl_4+2CH_3CN+9H_2 = 4TiC_{0.5}\,N_{0.5} + 2CH_4 +16HCl \qquad (3)$$

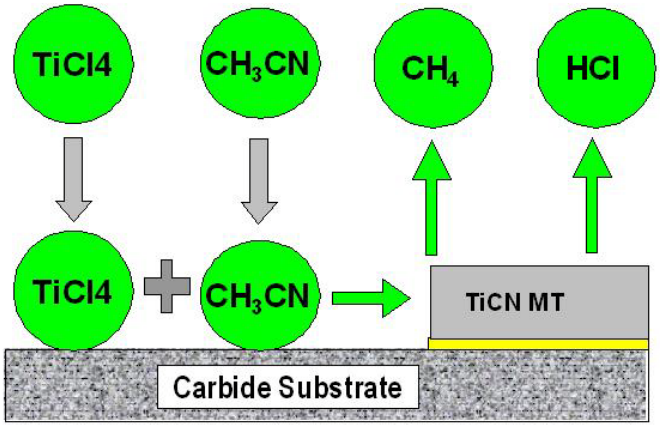

Figure 8: Schematic drawing of MT-TiCN deposition on a TiN layer.

The gaseous components $TiCl_4$ and CH_3CN are passed over the substrate to be coated, at a specific temperature. Solid MT-TiCN formation requires a number of thermodynamic requirements to be met. The direction of the reaction sequence is determined by the enthalpy of the reaction ΔH, which is dependent on temperature. When ΔH is negative, the reaction in the equation is displaced to the right.

SEM investigations of MT-TiCN coatings on TiN showed a columnar microstructure with large faceted grains which were not equiaxed but had an average long axis of about

© Technion - Israel Institute of Technology, Elyachar Central Library

9µm and a short axis of 1µm [10, 21, 28]. The properties of MT- TiCN were widely investigated to improve the coating performance by adding new process gases. Ruppi investigated MT-TiCN coatings by adding carbon monoxide (CO) [29]. This resulted in grain refinement of the MT-TiCN and a higher hardness (from 2640 to 3200 Hv). With increasing CO doping, the surface smoothness was improved and friction was reduced. However, cutting tests showed a lower wear resistance.

2.3.1.3 Thermal cracks due to residual stress

The chemical stability and hardness of CVD coated carbide tools are better than that of uncoated carbide substrates. However, the fracture toughness of CVD coated carbide tools is not as good as that of the uncoated carbide substrate. Experimental results showed that the failure of coated carbide tools is mainly caused by the formation and extension of surface cracks [41].

The first mechanical problems of CVD coatings may occur as soon as the coating is deposited on the substrate. In the absence of any external mechanical stress, the elastic interaction between the coating and substrate generates mechanical stress, commonly referred to as "residual stress". Residual stress is generated throughout the coating and substrate system [22].

Residual stresses are generated in most coatings as a result of the manufacturing process. They can be a result of growth mechanisms or, if there is a mismatch in thermal expansion between the coating and substrate material, significant stresses can build up during cooling from a high deposition temperature. Usually, residual stresses result from both sources [32]. Residual stresses in a coating and substrate system have two components, one thermoelastic and the other intrinsic. These components can cause thermal cracking .

With increasing coating thickness the main purpose of the substrate is to support the coating and to provide crack arrest to prevent failure, if and when thermal cracks

© Technion - Israel Institute of Technology, Elyachar Central Library

penetrate the coating [10]. Improvement in crack resistance of TiCN-MT coatings by changing deposition conditions should be investigated.

Thermoelastic stresses are generated during a change from the deposition temperature, to another temperature. The difference between the thermal expansion coefficients of the coating and substrate cause deformation to occur. Examination of CVD coated inserts indicates that they susceptible to spontaneous mechanical damage. Regarding the damage mechanisms, spontaneous cracking and coating detachment may occur in the different stages of a film formation [13].

Coated substrates generally becomes mechanically unstable when the stored elastic energy corresponds to the bulk fracture energy of the coating (Figure 9). As the crack spreads through the thickness of the coating, it may produce plastic deformation of the substrate when it reaches the interface (Figure 9a), can be deviated at the interface and cause the coating to become detached (Figure 9b), or propagate inside the substrate (Figure 9c). These failures may limit any further application. For example, machining under interrupted conditions requires mechanically stable inserts. Otherwise, sudden fractures of the coated insert can occur.

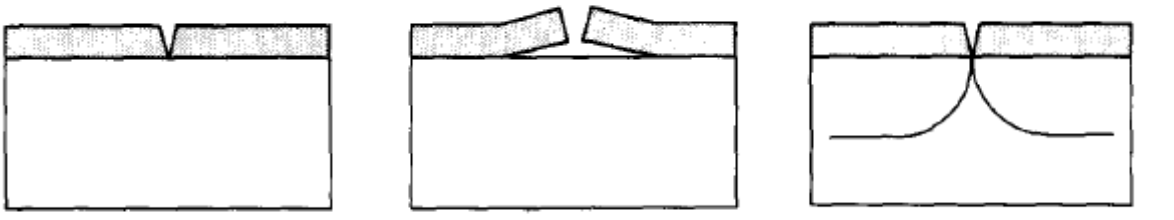

a. Tensile stress cracking

b. Tensile stress cracking and delamination

c. Tensile stress cracking and failure of the substrate

Figure 9: Schematic representation of various types of failure [15].

2.4 Importance of coating thermal stability in wear processes

The influence of oxidation can drastically affect the performance of cutting inserts working at temperatures higher than 600°C [39]. In general the oxidation behavior depends on the coating stoichiometry and microstructure, the substrate temperature and the oxidation environment.

© Technion - Israel Institute of Technology, Elyachar Central Library

During the cutting process, coatings interact with the working environment that leads to loss of material by the process known as wear. Therefore, the composition and properties of the coatings should be such as to resist wear in the working high temperature environment during the designed life period. Material loss through wear is negligible as long as the required coating composition and coating integrity can be achieved.

At the rake face where the cutting temperature is the highest, chemical wear dominates [21]. The mechanical properties of TiCN MT coatings could very easily be reduced by the formation of titanium oxide (Ti_xO_y). This layer is formed due to the high affinity of oxygen to titanium [29]. The difference between the thermal expansion coefficients of metal (TiCN-MT) and oxide (Ti_xO_y) develop stresses within the oxide layer and can cause spallation of the oxide layer from TiCN-MT coating. This mechanism of coating oxidation can reduce insert tool life dramatically.

The influence of TiN coatings on the properties of WC-based cemented carbides was reported by Igarashi [8]. It was found that TiN coatings increased the strength and oxidation resistance. In steel cutting, it improved chipping and thermal crack resistance but reduced crater wear resistance. The oxidation resistance of TiCN-MT should be improved in order to reduce oxidation rate and thus increase insert tool life.

2.5 Tribological Properties

The wear process is very complex, involving both mechanical and chemical interaction between the contacting surfaces and is to a large extent governed by the cutting forces, the cutting speed and the chemical composition of the coating and the raw materials, respectively. As mentioned before, coated cemented carbide is the dominant tool material for metal cutting operations [9]. The thickness of the coatings is one important key to improving their ability to protect the substrate against wear, oxidation, and corrosion; increasing the coating's thickness extends their useful life as a protective barrier [27].

© Technion - Israel Institute of Technology, Elyachar Central Library

One of the processes responsible for the wear of materials is friction. Wear is caused by interactions of cutting inserts with the raw material in the surrounding environment. The general form of the wear equation stipulates that wear volume is directly proportional to the hardness of the surface [14].

Wear of a material occurs at the surface exposed to the working environment. The definition does not include loss of dimension from plastic deformation, although for all practical purposes, wear has occurred despite material removal. In abrasive wear, the most important parameter is the hardness of the abraded material [14,31].

2.5.1 Cutting tests

It was found that machining is a complex process where several wear and failure mechanisms interact. This interaction must be taken into account when developing an insert geometry, substrate and coatings for a specific application. The main parameters defining the properties of the cutting insert are high hardness and chemical inertness of the coated insert. In wear applications, high hardness and low frictional properties are general requirements for good performance [11]. These parameters are essential for reducing abrasive and adhesive wear [10].

At the insert rake face (top side) where the cutting temperature is the highest, chemical wear dominates. At the insert flank face mechanical wear dominates [10]. All cutting tools wear during machining, and continue to do so until they come to the end of their tool-life. The life of a cutting edge is counted in minutes. Tool-life is the productive time available during which the edge will machine components, to be acceptable within the limiting parameters of cutting conditions.

The cutting edge of an insert used in a continuous cutting operation is considered worn out when it can no longer generate a certain surface morphology. Wear of the insert nose means the insert needs changing. In interrupted operation, fracture of the insert nose will stop the machining process. The tool-life may be limited when the edge loses its chip

© Technion - Israel Institute of Technology, Elyachar Central Library

control ability or when the wear pattern has developed to a stage where the risk for rapid edge breakdown is imminent.

The classification of tool wear types has been developed to form an important base line for assessing the machining operation and to optimize productivity by getting the tool grade and machining conditions right for the type of cut and material. The criteria of machining, i.e. economics accuracy, removal rate, surface morphology and chip control, depend on the development of tool wear.

By inspecting the magnified cutting edge and acting upon what the wear pattern indicates, the useful tool-life of the cutting edge can be controlled, extended and relied upon. There is always an ideal wear development for an operation. For example, flank and crater wear (Figure 10(1-2)) is typical failure during continuous cutting conditions and insert nose fracture (Figure 10(8)) during interrupted conditions.

At the rake face, compared with the flank face, the temperature in the workpiece material (the chip) is high, and the workpiece material can be considered relatively soft, and abrasive wear is not as pronounced [36]

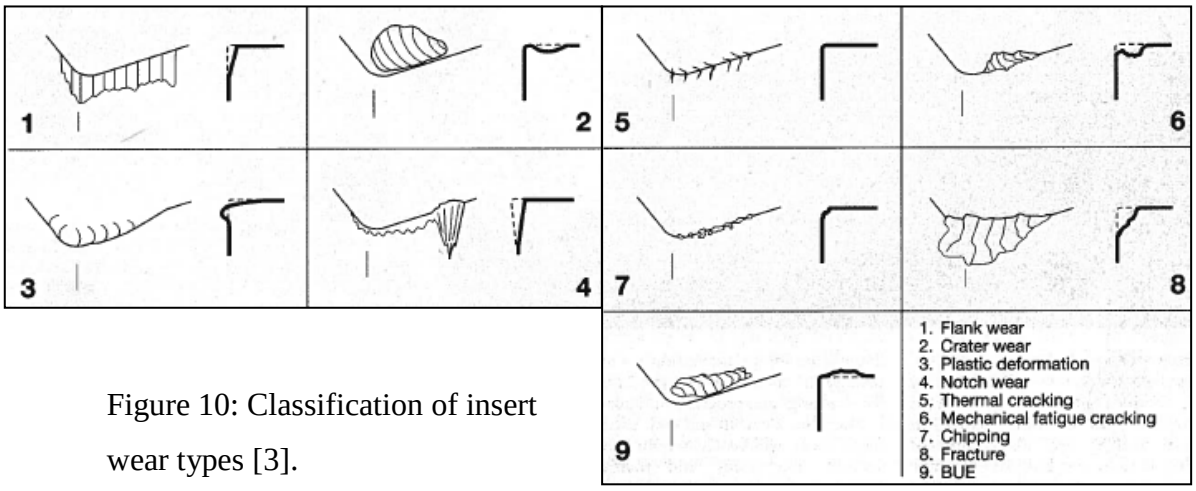

Figure 10: Classification of insert wear types [3].

The choice of the right tool or the right coating in a specific machining operation is not an easy task. To select the right tool one was to take into consideration the material of the

workpiece, the machining conditions and the actual machining method, which all together determine the mechanical and thermal stress of the cutting tool [31].

© Technion - Israel Institute of Technology, Elyachar Central Library

© Technion - Israel Institute of Technology, Elyachar Central Library

2.6 Research goals

The first generations of coated metal cutting inserts had several limitations that restricted a more general application in metal cutting. Firstly, the relatively high deposition temperature (~ 850 - 950^{o}C) during CVD results in diffusion of substrate elements into the coating during growth. The main effect is embrittlement of the cutting edge and reduction of adhesion, especially if significant amounts of the brittle η-phase are formed near the substrate-coating interface. It is generally accepted that MT-TiCN coatings have a columnar microstructure, but to our knowledge no detailed study of the growth, microstructure and mechanical properties of these coatings has been presented.

The main objective of this study is to investigate MT-TiCN coatings using different deposition conditions (in this case deposition temperature, pressure and hydrogen flow range) and to evaluate their influence on texture and mechanical properties.

© Technion - Israel Institute of Technology, Elyachar Central Library

3 EXPERIMENTAL METHODS AND PROCEDURES

3.1 Coatings experiments

MT-TiCN coatings investigated were deposited using a computer-controlled hot-wall CVD reactor. Commercial cemented carbide inserts (CNMG 432GN) with a composition of WC-93.5wt.%, Co-6wt.% and (Ta,Nb)C-0.5wt.% were used as substrates. The experimental coatings were deposited on a TiN adhesion layer.

3.1.1 Design of Experiments

In this research JMP-DOE software was used to provide comprehensive statistics and an interactive environment for designing experiments, analyzing and exploring data, and uncovering trends that might otherwise go unnoticed.

Designing experiments is centered on three factors which influence deposition:

- Temperature (range 775^{o}C - 975^{o}C)
- Process pressure (range 60 -120 mbar)
- H_2 flow (range 33 - 50 L/min)

Parameters of the coating deposition range were suited to the machine and process limitations. According to these coating deposition parameters, a list of trial runs determined using JMP-DOE (Table 1).

© Technion - Israel Institute of Technology, Elyachar Central Library

exp. #	Temp. [^{0}C]	Pressure [mbar]	H_2 [L]	$TiCl_4$ [ml]	CH_3CN [ml]
ref.	875	90	33		
exp. # 1	975	120	33		
exp. # 2	975	60	33		
exp. # 3	875	90	42		
exp. # 4	975	60	50	const.	const.
exp. # 5	775	60	33		
exp. # 6	775	60	50		
exp. # 7	775	120	50		
exp. # 8	775	120	33		
exp. # 9	975	120	50		

Table 1: Schedule for trial deposition conditions.

A schematic 3D presentation of deposition parameters ranges can help in understanding the experimental scatter. As in Figure 11, every point in space represents an entire region. After result analysis, these ten experiments will represent the coating properties and coating behavior throughout the experimental space.

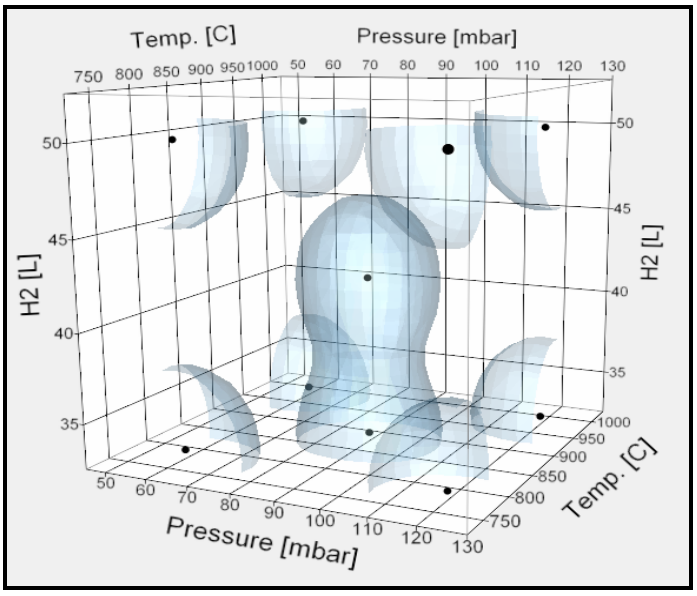

Figure 11: Schematic presentation of deposition parameter range used in this study.

© Technion - Israel Institute of Technology, Elyachar Central Library

3.1.2 Sample preparation

Cleaning the surface of inserts (substrate) is an essential step for good coating adhesion. The goal of the cleaning processes is to rid inserts surface from pollutants from prior to coating steps. The cleaning process is divided into two main steps. In the first step, primary cleaning by wet sand blasting, large unwanted particles are removed. The second step is to remove micro particles using ultrasonic energy in an ultrasonic bath.

The industrial cleaning machine (Figure 12) is able to finish these two steps in a few minutes.

Figure 12: Machine for inserts preparation before coating.

3.1.3 Loading method

The inserts were loaded on graphite plates (Figure 13). These plates are resistant to the high temperature process. Plate loading provides uniform thickness distribution.

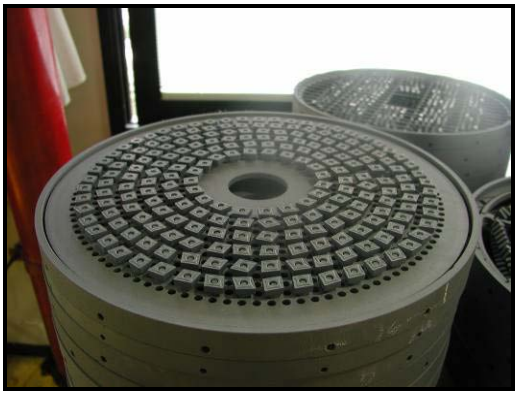

Figure 13: Insert loading method for uniform thickness distribution.

© Technion - Israel Institute of Technology, Elyachar Central Library

3.1.4 Deposition process

TiCN-MT trial coatings (Table 1) were deposited onto standard cemented carbide tool inserts using a Bernex 530L CVD system (Figure 5). Precursors used were $TiCl_4$, CH_3CN and H_2 for balance. The purity of the gases and reactants used in the experiments was 99.9995%. The deposition temperature range was 775°C - 975°C; process pressure in the range of 60 -120 mbar; and H_2 flow in the range of 33-50 L/min. Precursor flow rates were monitored by mass flow and liquid flow controllers. The pressure was maintained by a rotary vane vacuum pump. Cold traps were used to collect the by-products. Chloride and cyanide containing compounds were neutralized in an alkaline solution. The CVD reactor, with graphite heating elements (hot wall design), was equipped with its own scrubber system for effluent treatment.

Deposition of all coatings started with a TiN base layer that was ~0.5µm thick. Figure 14 presents the temperature and pressure cycles.

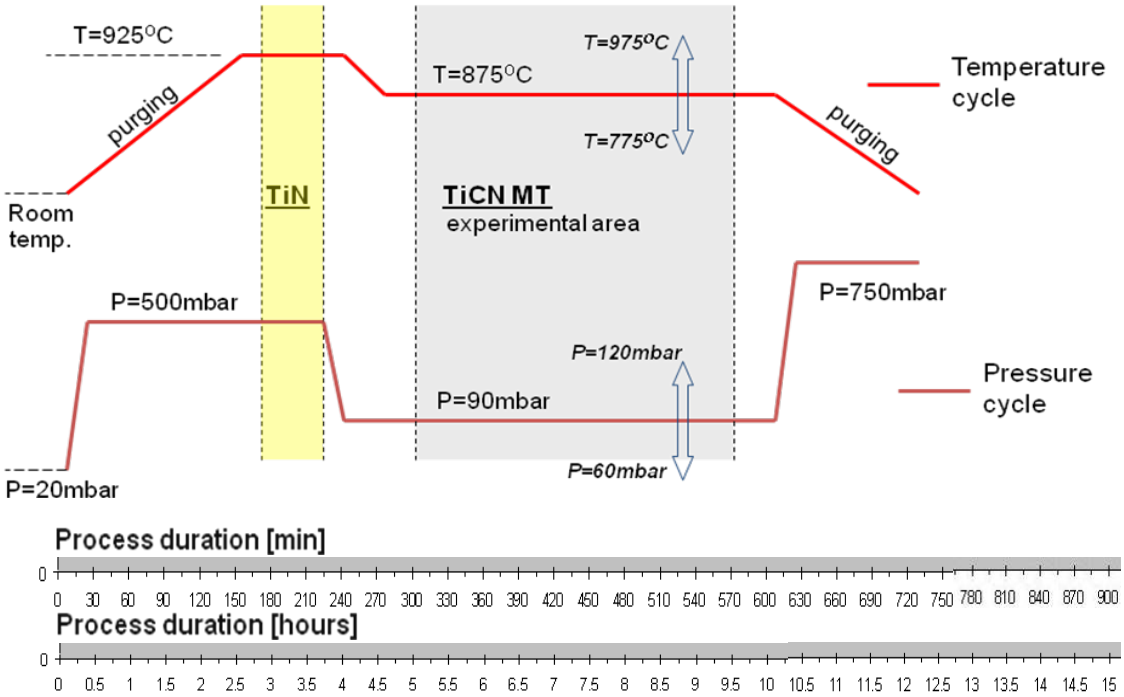

Figure 14: Schematic presentation of the deposition process.

© Technion - Israel Institute of Technology, Elyachar Central Library

For deposition of TiCN-MT, the reacting gases ($TiCl_4$, CH_3CN and H_2) were carried by separate lines and then mixed before entering the reactor. In this setup, hydrogen was used as the carrier gas to transport titanium tetrachloride and azetonetril into the reaction zone. After the reacting gases enter the reactor, they gradually reach the deposition temperature and by favoring the thermodynamic conditions for the reaction, the coating is deposited on the substrates surfaces.

3.2 Optical investigation

3.2.1 Coating Thickness Measurement

The coating thickness was measured using a Reichert – Jung optical microscope. The inserts were mounted and polished for proper coating thickness measurement. The polishing steps used standard sets of diamond solution: diamond particles of 45µm, 15µm, 6µm and 1µm. Coating thicknesses were evaluated by measuring the coating thickness of three inserts.

3.2.2 Thermal cracks

White light was used for crack detection. The surface must be highly polished to allow adequate light reflection for detection of the crack lines. Polishing was carried out on a flat rotating disc using 6µm, 3µm and 1µm diamond particles.

3.3 Evaluation of the Microstructure

The microstructures of the coatings were characterized using scanning electron microscopy (SEM). Texture was determined by various methods including X-ray diffraction and electron backscatter diffraction (EBSD).

3.3.1 Scanning Electron Microscopy (SEM) Investigation

The experimental coatings were studied by SEM using Jeol - JSM6500F instrument. For examination of the fracture of the coating, the inserts were broken by impact load. For

© Technion - Israel Institute of Technology, Elyachar Central Library

examination of insert surface morphology, no special sample preparation is required. SEM coating characterization was done at an accelerating voltage of 15kV, an emission current of 104μA, and a working distance (WD) of ~ 8mm.

3.3.2 X-ray Diffraction Analysis (XRD)

In order to identify the crystalline phases present in the coatings, X-ray diffraction (XRD) analysis was performed using a Philips - X'Pert pro diffractometer with Cu Kα radiation. Preferred orientation (texture) of the TiCN-MT coatings was determined using Equation (4),

$$P_{hkl} = \frac{I(hkl)}{I'(hkl)} \cdot \frac{\sum I'(hkl)}{\sum I(hkl)} \qquad (4)$$

where I (hkl) is the measured integrated intensity of the (hkl) reflection; I'(hkl) is the reflection intensity for a completely random sample.

When a distribution of grains is totally random, P=1. Powdered TiCN coating on glass was used as reference. If the grain orientations of the experimental coatings are textured, the deviation of the different intensities from that of the random powder sample can be used to determine the average grain orientations. P>1 indicates a preferred orientation for the reflection hkl. For preferred orientation measurements milled TiCN coating was used.

The use of XRD for preferred orientation analysis is limited, in that it is difficult to use XRD on a small selected area of a polycrystalline surface. Recently, alternative techniques for localized orientation measurements have been developed, such as electron backscatter diffraction (EBSD). EBSD is a highly flexible method to measure grain orientation distributions [19,20]. The method allows direct examination of the individual grains, grains boundaries and the orientation of each individual crystal. In this research SEM was used to characterize the morphology of crystals. XRD and SEM-EBSD were used for preferred orientation analysis.

© Technion - Israel Institute of Technology, Elyachar Central Library

3.3.3 Texture analysis by SEM-EBSD

In this work, electron backscattering diffraction (EBSD) was utilized to determine the individual grain orientations using mapping technique. SEM-EBSD from Oxford Instruments installed on a FEI E-SEM Quanta 200 was used for grain orientation detection.

Orientation mapping

EBSD can be used to find the crystal orientation of the material located within the incident electron beam's interaction volume. Thus, by scanning the electron beam in a prescribed fashion (typically in a square grid) results in a map of local orientation. These maps can spatially describe the crystal orientation of the material being investigated and can be used to examine micro-texture and sample morphology. Various statistical tools can be used to measure the average misorientation, grain size, and crystallographic texture.

Texture was represented using pole figures, in which a specified crystallographic axis (or pole) from each of a representative number of crystallites is plotted in a stereographic projection. In order to get orientation map data from EBSD analysis, good sample preparation is essential. Otherwise, the resulting EBSD patterns will be of poor quality or will not be visible at all.

Sample preparation method

Most of the samples required some degree of mechanical polishing. There are three steps to a complete sample preparation: sectioning, tripod mounting, and polishing. Sectioning removes a representative area from a parent specimen. The sample must be small enough for its mounting in the pyrex holder. The limiting factor for the sample size is the diameter of the pyrex holder seated in the tripod. The specimen was mounted onto the pyrex holder with wax. The polishing steps used standard sets of diamond solution with diamond particles ranging from 45 µm to 1 µm. Colloidal silica of 0.05 µm was used in the last polishing step. After polishing, the sample was removed from the pyrex holder using acetone.

© Technion - Israel Institute of Technology, Elyachar Central Library

3.3.4 Stylus instrument for Surface Roughness Measurements

The morphological features of the surface of both macro-levels and micro-levels are important factors governing the wear and corrosion behavior of the material. On the macroscale, the surface roughness or general topography of the surface can be considered as the index for surface morphology.

The roughness measurements were done using a Mahr Perthometer S2 instrument. The method is based on a stylus that is connected to a transducer, which gages the depth of surface roughness. The mechanical impulses of the stylus movement are converted into electrical impulses in the transducer. An amplifier is used to boost the electrical signal. Recording and data logging systems are used for information storage and presentation. The stylus movement over the surface is controlled through a gearbox. The average roughness (Ra) was determined from:

$$R_a = \frac{1}{L}\int_0^L |z| dx \qquad (5)$$

where: L is the length of the linear segment on the surface, and z is the surface height at position x.

3.4 Evaluation of Mechanical Properties

3.4.1 Nano-hardness measurements

The term nano-hardness refers to a measurement of hardness at such low loads as to limit the size of the indentation to within the coating. The relatively shallow penetration of the indenter, with a low load, allows for determination of the hardness of a thin coating. The load must be sufficiently small so as to affect the coating and not the substrate. Surface polishing with 1 μm diamond film was carried out for all experimental coatings. This preparation enabled to minimize scatter in the data.

Nanoindentation testing was carried out using a CSM nano-indentation tester with a Berkovich indenter. The indenter tip geometry and machine compliance were carefully

© Technion - Israel Institute of Technology, Elyachar Central Library

calibrated prior to testing using a fused silica standard, and the load-displacement curves were analyzed to generate hardness data. All the load-displacement curves were inspected prior to analysis, and those with large pop-ins and discontinuities in the loading or unloading curve were not included in the analysis.

Optical microscopy was used for selecting a specific sample site prior to indentation and for checking the location of the imprint after indentation. The microscope is directly linked by an electro-mechanical positioning system which allows movement along two perpendicular horizontal axes. After area selection, the indentations were made at 135mN load. The load was directly applied by an electromagnet assembly to a vertical rod, the end of which houses a standard Berkovich diamond indenter. The measuring load was chosen to be low enough so that the measuring head does not penetrate through the coating. The maximum depth of the indentation must be lower than 10% of total coating thickness to avoid influence of the substrate [31]. At least 20 indentations were selected for each coating and the results were averaged.

3.4.2 Evaluation of the adhesion

Adhesion properties of wear resistant CVD coatings on cutting inserts are essential to their performance in machining. Moreover, at the substrate/coating interface, strains are generated due to different thermal expansion coefficients and different elastic properties between the substrate and coating [38]. It is therefore necessary to characterize the coating adhesion by an appropriate measurement technique.

Indentation methods are nominally suited for qualitative adhesion investigations. The advantage of this method is that it is easy to use, even in an industrial environment[11]. The principle of such tests involves imposing a mechanical stress at the interface either through the coating or substrate and then detecting interface failure, if it happens. Adhesive failure occurs when the fracture is at the interface between the substrate and coating. If fracture occurs in the substrate or in the coating, the failure is called cohesive failure. In this study adhesion was qualitatively analyzed using a load of 20kgF with a Vickers indenter.

© Technion - Israel Institute of Technology, Elyachar Central Library

3.5 Thermal stability

The influence of oxidation can drastically affect the performance of cutting tools working at temperatures higher than 600°C [42]. Coating oxidation can generate a volumetric expansion, resulting in local loss of adhesion.

3.5.1 Measurement of resistance to oxidation

In order to exam the resistance to oxidation, oxidation tests were conducted in an open air furnace at temperatures of 800 °C using a Nabertherm laboratory furnace. The coated samples were held at this temperature for 60min and the oxidation rate was determined by oxide layer thickness measurement (every 15 min). Accordingly, four samples were used for each type of coating. After heat treatments, the samples were kept at room temperature. For each experiment, the oxidation thickness of the coatings, as a function of exposure time, was measured using SEM (Figure 15).

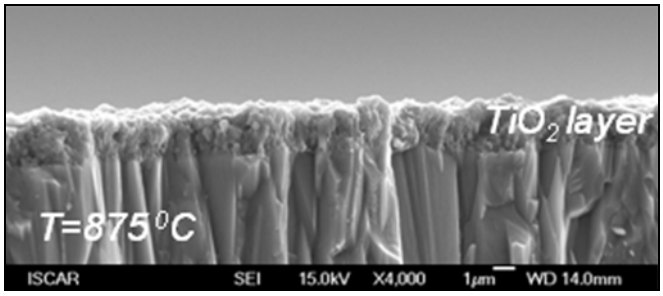

Figure 15: Oxidation layer (TiO_2) thickness measurement by SEM.

3.6 Tribological properties

Cutting tests in the form of continuous and interrupted turning of a carbon steel (AISI 1060 and AISI 4340) were performed in order to evaluate the performance of the coated inserts. The cutting times were chosen to follow the flank and crater wear progress.

3.6.1 Interrupted cutting test on AISI 1060

Interrupted cutting tests were designed to evaluate insert resistance to deformation and fracture. Under specific cutting conditions the insert should fail due to sudden fracture and not wear development. Interrupted cutting tests were applied on AISI 1060 using following conditions:

© Technion - Israel Institute of Technology, Elyachar Central Library

- cutting conditions: Vc=150[m/min], f=0.2[mm/rev], A=2[mm], dry (without cooling)
- insert geometry: CNMG 432GN
- raw material shape (see Figure 16)

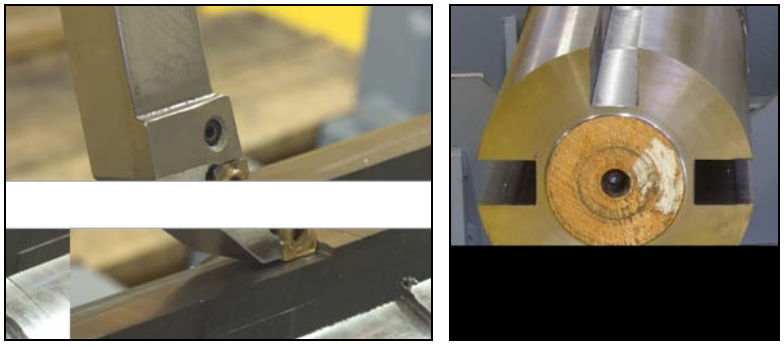

(a) top view. (b) side view.

Figure 16: Photographs of the raw material (AISI 1060) used for interrupted cutting tests.

3.6.2 Continuous cutting test on AISI 1045

Continuous cutting test were designed to evaluate insert resistance to flank and crater wear (Figure 10). Under specific cutting condition the insert should fail due to developed wear and not sudden fracture. Continuous cutting test was applied on AISI 1045 under following conditions:

- cutting conditions: Vc=250[m/min], f=0.2[mm/rev], A=2[mm], wet (with emulsion cooling).
- insert geometry: CNMG 432GN
- raw material shape (see Figure 17).

The cutting times were chosen to be 8,14,16,18 and 20 min in order to follow the flank and crater wear. After the abrasion test the worn inserts were subjected to careful examination using optical microscopy in order to evaluate the dominant wear mechanisms.

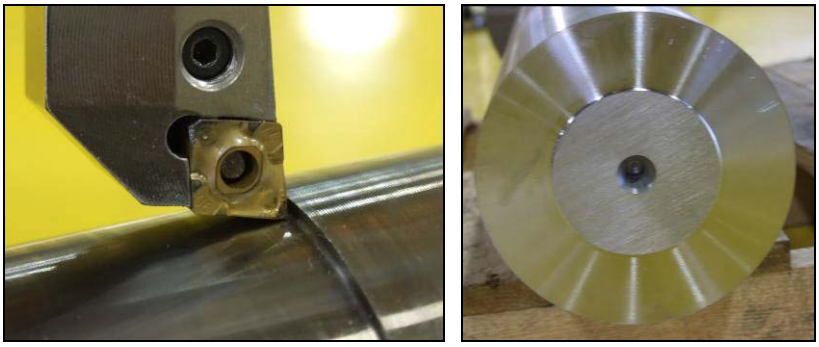

(a) top view. (b) side view.

Figure 17: Photographs of the raw material (AISI 1045) used for continuous cutting tests.

© Technion - Israel Institute of Technology, Elyachar Central Library

© Technion - Israel Institute of Technology, Elyachar Central Library

4 RESULTS

4.1 Evaluation of the Microstructure

4.1.1 Scanning Electron Microscopy (SEM) Results

SEM showed that the TiCN MT experimental coatings have a columnar grain morphology (see Figure 18).

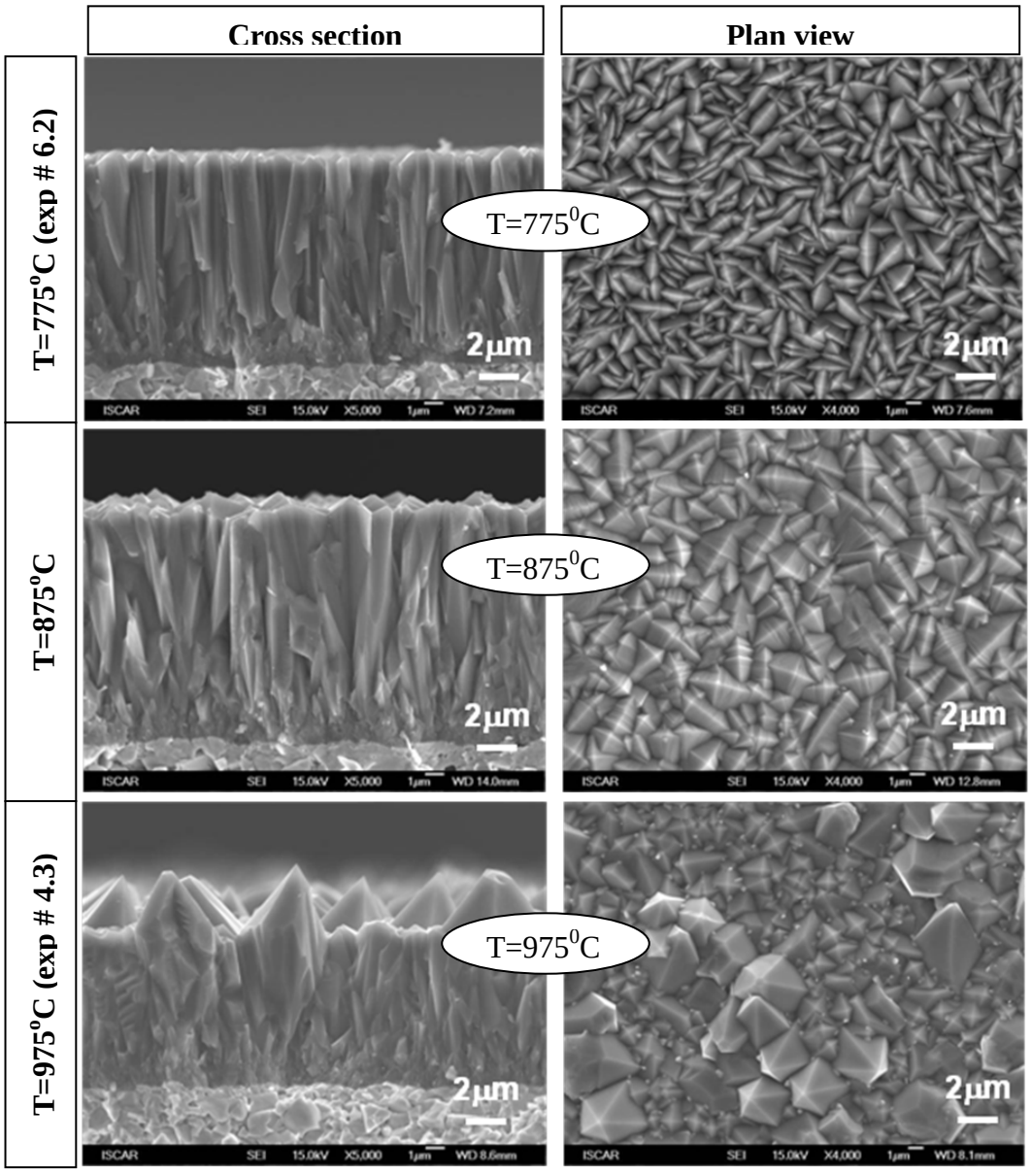

Figure 18: SEM micrographs of the coating microstructure as a function of process temperature.

© Technion - Israel Institute of Technology, Elyachar Central Library

The columnar grain growth was inspected at temperatures ranging from 775 to 975 ^{o}C. It was found that coating deposition at high temperatures leads to a coarse microstructure nucleation within a fine columnar matrix. The coarse grains have a five-fold symmetry and a growth rate higher than that of the other grains. A comparison of grain growths is presented on cross section image of experiment #4.3 (Figure 18). On the other hand, low temperature deposition leads to fine, uniform columnar grains growth, experiment #6.2. SEM-EBSD analysis was then done in order to investigate structure variety as a function of process temperature.

4.1.2 SEM-EBSD Results

SEM-EBSD analysis determined that these five-fold microstructures consist of five grains (Figure 19). Moreover, mapping of the grain orientation using an inverse pole figure showed additional data regarding the grain orientation. Inverse pole figure measurements found that all five grains have the same orientation normal to the substrate {110} (Figure 20).

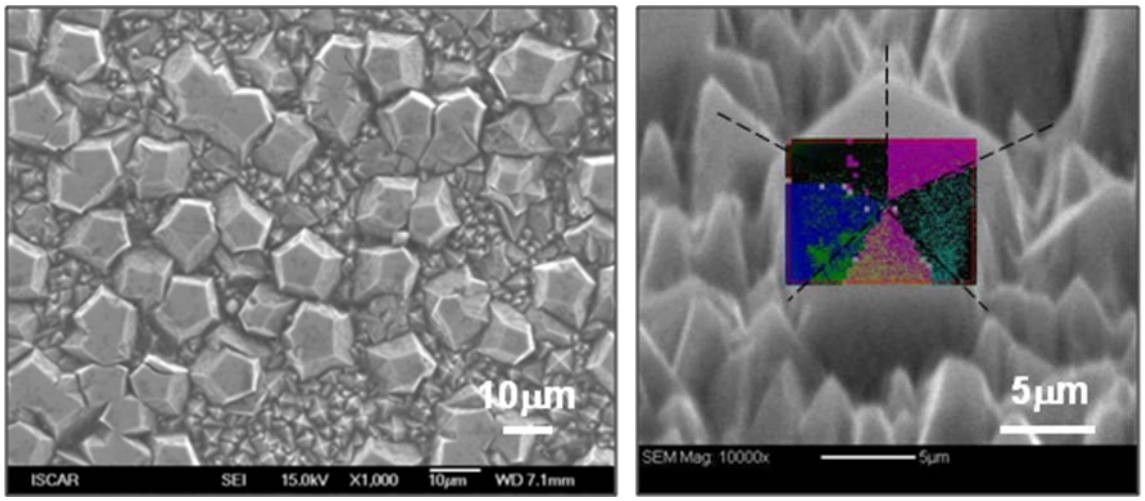

(a) (b)

Figure 19: Five-fold grains identification by SEM-EBSD analysis. (a) plan-view of polished five-fold structures. (b) SEM-EBSD pattern that provides distribution map of grains orientation.

© Technion - Israel Institute of Technology, Elyachar Central Library

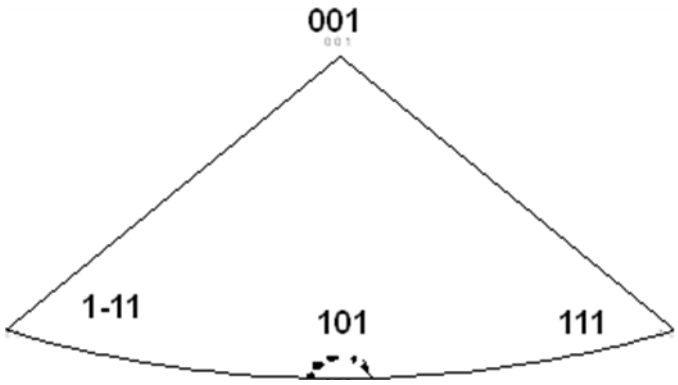

Figure 20: Specified crystallographic direction of selected five-fold structure measured by inverse pole figure.

4.1.3 X-ray Diffraction Analysis (XRD)

XRD analysis was done for all experimental coatings. Determination of preferred orientation (P) for the coatings is essential to understand the correlation between coating deposition conditions and microstructure. Table 2 presents the XRD results as a function of deposition parameters; temperature (T), pressure and hydrogen flow rate (H_2). The results are summarized according to the coating experiments schedule, from exp.#1 to exp.#9.

exp. #	Temp. [°C]	Pressure [mbar]	H_2 [L]	P (111)	P (200)	P (220)	P (311)	P (331)	P (420)	P (422)
ref.	875	90	33	0.1	0	0.3	2.6	1.1	0.4	3.8
exp. # 1.3	975	120	33	0.4	0.2	3.1 ●	1.1	1.5 ●	1.2	0.7
exp. # 2.2	975	60	33	0.3	0.1	3.1 ●	1.2	2 ●	0.7	1.4
exp. # 3	875	90	42	0.2	0	0.3	2.2	0.7	0.5	3.8
exp. # 4.3	975	60	50	0.3	0.1	3.1 ●	0.9	2.7 ●	0.5	1.2
exp. # 5.3	775	60	33	0.7	0.1	0.7	3.5 ●	1.7	0.7	3.8 ●
exp. # 6.2	775	60	50	0.4	0	0.4	2.6 ●	1.5	0.6	3.8 ●
exp. # 7.2	775	120	50	0.6	0.1	0.3	3.6 ●	2.4	0.7	3.8 ●
exp. # 8.2	775	120	33	0.2	0	0.1	2 ●	1.2	0.3	3.8 ●
exp. # 9.2	975	120	50	0.6	0.2	3.1 ●	0.9	2.5 ●	0.9	1.5

● T = 775°C
● T = 975°C

Table 2: Preferred orientation of the CVD experimental coatings.

Evaluation of the XRD data confirmed that deposition temperature plays an important role in the formation of the microstructure. A strong correlation between low temperature

© Technion - Israel Institute of Technology, Elyachar Central Library

deposition and grain growth parallel to [311] and [422] directions was found. On the other hand, a high deposition temperature leads to formation of more grain with [220] and [331] parallel to the substrate.

JMP-DOE was used to help understand how the deposition parameters (T, pressure, H_2), presented in Table 2, affect preferred grain orientation. For statistical analysis of the results (Table 2) a few statistical terms should be defined.

- Pareto Plot: a statistical technique in decision making that is used for selection of parameters which produce a significant effect on coating properties. The "importance" of each bar, process parameter, is given by its height, so we can make the plot easier to interpret by simply sorting the bars from largest to smallest.
- Factorial Model: helps to find how the results change as deposition parameters are changed.
- R-square (RSq): a measure of degree of a statistical model fit, from 0 (no fit) to 1 (exact fit).

<u>P (220) results analysis (RSq=0.83)</u>

Pareto plot analysis shows (Figure 21) that process temperature has a significant influence on the quantity of grains in a (220) orientation. Other deposition parameters (pressure, H_2) have a negligible influence on grain growth in this direction.

The factorial model (Figure 22) presents the correlation between temperature and number of grains with a (220) orientation. It shows that more grains with a (220) orientation are observed as the CVD process increases.

Term	Orthog Estimate
Temp. [C](775,975)	1.218657
H2 [L](0,50)	0.104042
Pressure [mbar](60,120)	-0.078262
Temp. [C]*Pressure [mbar]	0.078262
Temp. [C]*Pressure [mbar]*H2 [L]	-0.055902
Pressure [mbar]*H2 [L]	0.055902
Temp. [C]*H2 [L]	0.011180

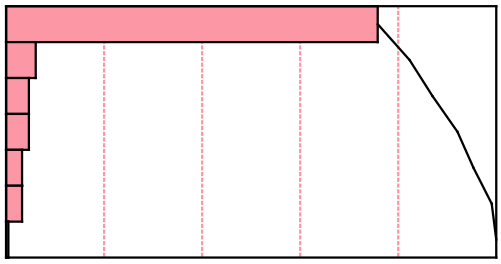

Figure 21: Pareto plot for (220) oriented grains.

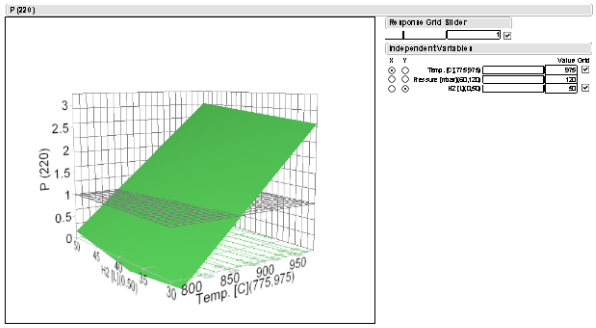

Figure 22: Factorial model for (220) oriented grains.

P (311) results analysis (RSq=0.96)

Similar to the P (220) results, Pareto plot analysis (Figure 23) presents a significant influence of temperature on the quantity of grains with a (311) orientation. Other deposition parameters (pressure, H_2) almost no have an influence on grains growing in the [311] direction.

The factorial model (Figure 24) presents the correlation between temperature and number of grains in a (311) orientation. As the CVD process temperature decreases, more grains with a (311) orientation are created.

© Technion - Israel Institute of Technology, Elyachar Central Library

Term	Orthog Estimate
Temp. [C](775,975)	-0.8497058
Pressure [mbar]*H2 [L]	0.2906888
Temp. [C]*Pressure [mbar]*H2 [L]	-0.2683282
Temp. [C]*H2 [L]	-0.1341641
Pressure [mbar](60,120)	-0.0670820
Temp. [C]*Pressure [mbar]	0.0447214
H2 [L](0,50)	-0.0351376

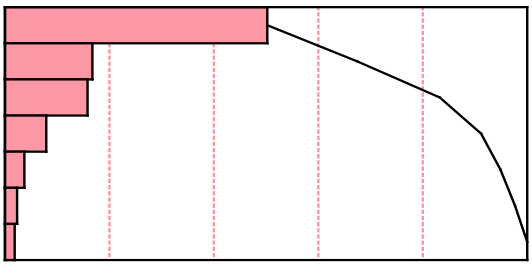

Figure 23: Pareto plot for (311) oriented grains.

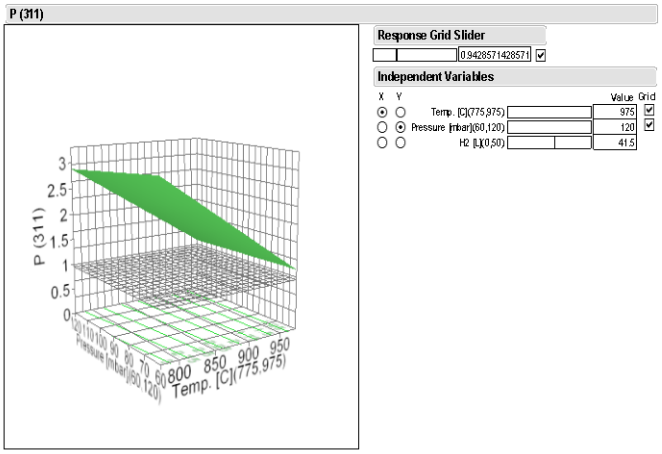

Figure 24: Factorial model for (311) oriented grains.

P (422) results analysis (RSq=0.84)

Similar to P (220) and (311) results, Pareto plot analysis (Figure 25) presents a significant effect of temperature on the amount of grains in a (422) orientation. Other deposition parameters (pressure, H_2), as in previous analysis, have a negligible influence on grain growth in this direction.

The factorial model (Figure 26) presents the correlation between temperature and number of grains in a [422] direction. As the CVD process temperature decreases, more grains with a (422) orientation are formed.

© Technion - Israel Institute of Technology, Elyachar Central Library

Term	Orthog Estimate
Temp. [C](775,975)	-1.162755
Pressure [mbar]*H2 [L]	0.111803
Temp. [C]*Pressure [mbar]*H2 [L]	0.111803
Temp. [C]*H2 [L]	0.067082
Pressure [mbar](60,120)	-0.044721
Temp. [C]*Pressure [mbar]	-0.044721
H2 [L](0,50)	-0.040122

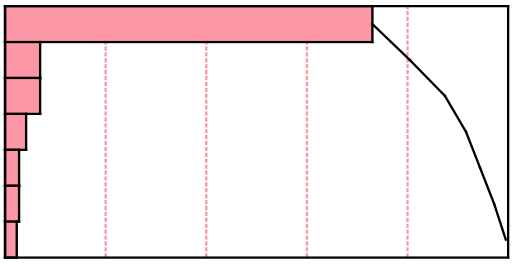

Figure 25: Pareto plot for (422) oriented grains.

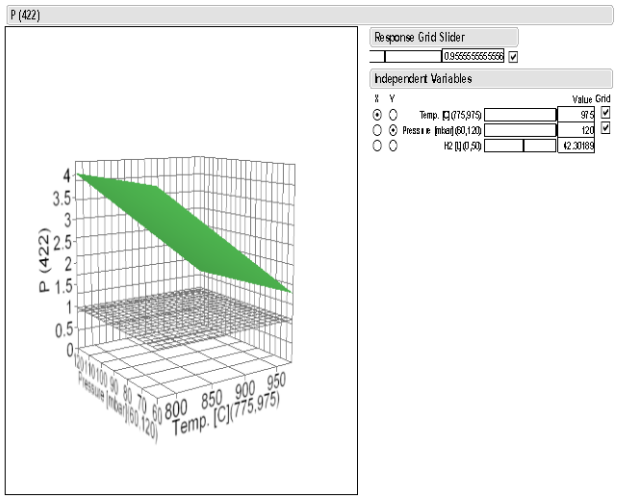

Figure 26: Factorial model for (422) oriented grains.

According to the statistical analysis, no correlation between T, pressure, H_2 and (331) oriented grains was found.

© Technion - Israel Institute of Technology, Elyachar Central Library

© Technion - Israel Institute of Technology, Elyachar Central Library

4.2 Optical Microscopy

4.2.1 Coating Thickness

The thickness of the coating was measured by optical microscope. Twenty one runs were made during the research. However, the large numbers of experiments resulted in a varying thickness. Therefore, additional experiments were required to correct the coating thickness. Only 10µm thick coatings were chosen for analysis of microstructure and mechanical properties. The coating thickness results of the trial selected coatings are summarized in Table 3.

run #	exp. #	Temp. [^{0}C]	Pressure [mbar]	H_2 [L]	$TiCl_4$ [ml]	CH_3CN [ml]	Process duration [min]	Thickness [µm]
1	ref.	875	90	33	const.	const.	300	12
4	exp. #1.3	975	120	33			290	6-10
6	exp. #2.2	975	60	33			300	11-15
7	exp. # 3	875	90	42			300	11
10	exp. #4.3	975	60	50			350	8-10.5
13	exp. #5.3	775	60	33			440	10
15	exp. #6.2	775	60	50			440	11.5
17	exp. #7.2	775	120	50			440	13
19	exp. #8.2	775	120	33			440	10
21	exp. #9.2	975	120	50			450	7-9

Table 3: Coating thickness results of selected experiments.

4.2.2 Thermal cracks

Cracks due to thermal expansion coefficient mismatch between the coating and substrate were found in all experimental conditions. All high temperature (875^{o}C, 975^{o}C) coated samples had wide open surface cracks. While the coatings deposited at relatively low temperature (775^{o}C) showed fine cracks, as presented in Figure 27.

Crack formation indicates residual stress in the samples. From these findings it can be concluded that the process temperature influences the generation of residual stresses.

© Technion - Israel Institute of Technology, Elyachar Central Library

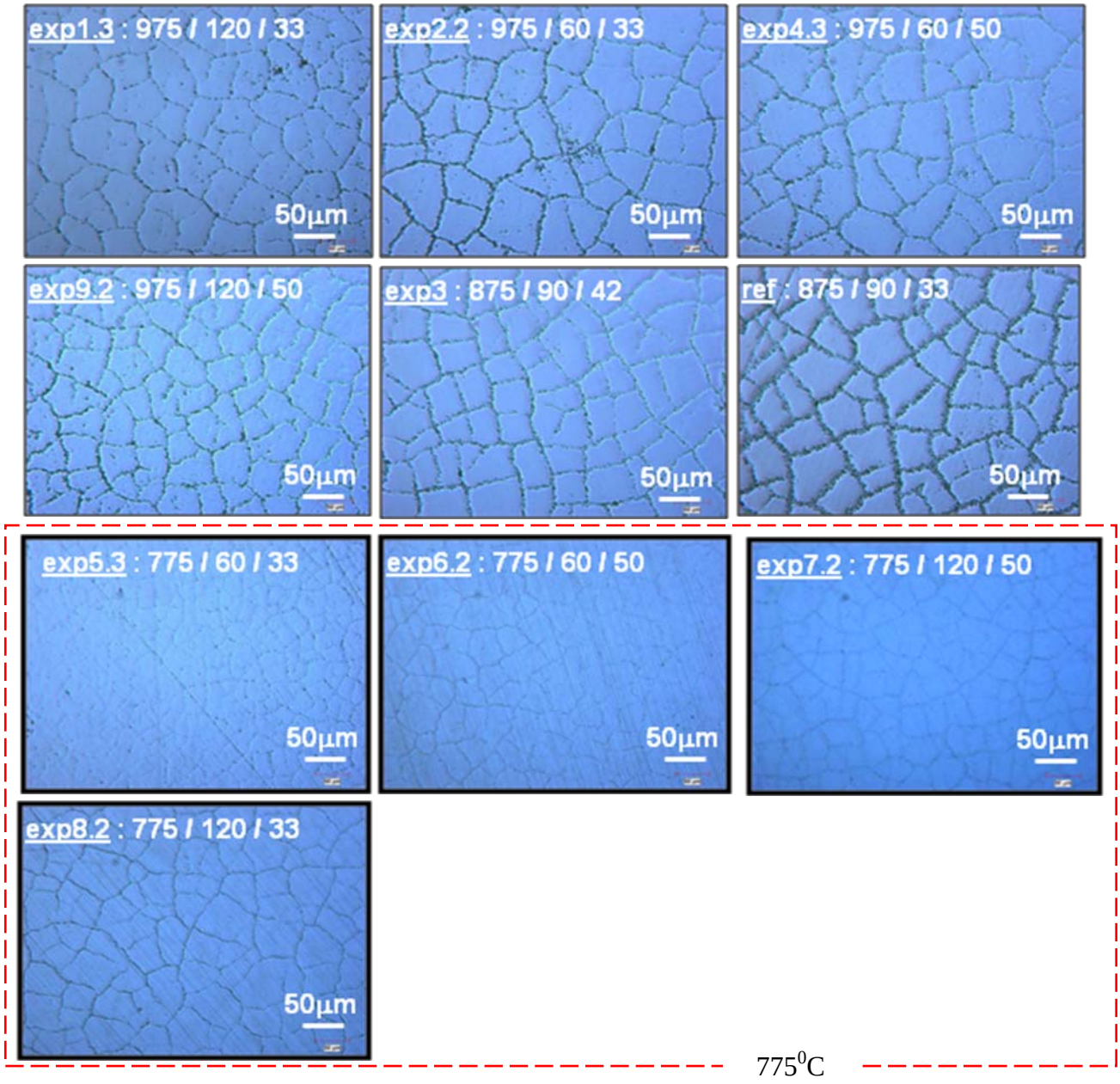

Figure 27: Plan-view of polished samples for thermal crack investigations.

© Technion - Israel Institute of Technology, Elyachar Central Library

4.3 Evaluation of Mechanical Properties

XRD, SEM and the results of thermal crack distribution indicate a significant influence of process temperature on coating microstructure.

4.3.1 Surface Roughness

The surface roughness results (Ra) are summarized in the Table 4, which is formatted according to increasing CVD deposition temperature.

exp #	Temp. [^{0}C]	Pressure [mbar]	H_2 [L]	Ra [μm]
exp. # 1.3	975	120	33	0.46 ± 0.03
exp. # 2.2	975	60	33	1.32 ± 0.05
exp. # 4.3	975	60	50	0.75 ± 0.09
exp. # 9.2	975	120	50	0.66 ± 0.05
exp. # 3	875	90	42	0.2 ± 0.05
ref.	875	90	33	0.19 ± 0.05
exp. # 5.3	775	60	33	0.14 ± 0.03
exp. # 6.2	775	60	50	0.2 ± 0.05
exp. # 7.2	775	120	50	0.19 ± 0.01
exp. # 8.2	775	120	33	0.17 ± 0.01

Table 4: Surface roughness of trial coatings.

It is clear from Pareto plot analysis (Figure 28) that process temperature has a significant effect on coating roughness. Other deposition parameters (pressure, H_2) have almost no influence on Ra.

Factorial model (Figure 29) indicates that Ra of the coating will increase with increasing process temperature. The results are in agreement with the SEM findings.

Term	Orthog Estimate
Temp. [C](775,975)	0.2806265
Temp. [C]*Pressure [mbar]	-0.1106854
Pressure [mbar](60,120)	-0.1017411
Temp. [C]*Pressure [mbar]*H2 [L]	0.0883247
Pressure [mbar]*H2 [L]	0.0838525
Temp. [C]*H2 [L]	-0.0480755
H2 [L](0,50)	-0.0089215

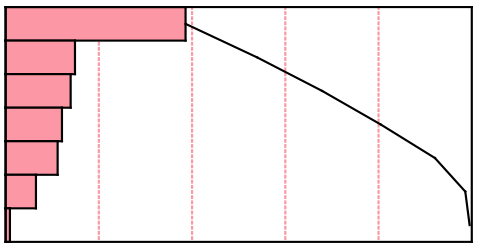

Figure 28: Pareto plot for roughness results.

© Technion - Israel Institute of Technology, Elyachar Central Library

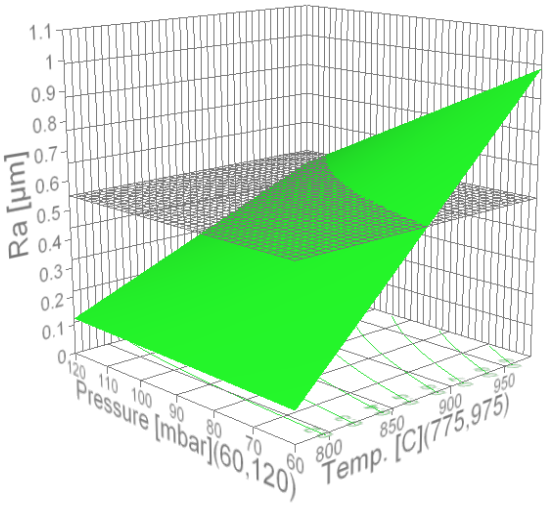

Figure 29: Factorial model roughness results.

4.3.2 Hardness measurements

Hardness measurements of the coatings are summarized in Table 5.

exp #	Temp. [^{0}C]	Pressure [mbar]	H_2 [L]	Hardness - Hv
exp. # 1.3	975	120	33	2310 ± 109
exp. # 2.2	975	60	33	2570 ± 167
exp. # 4.3	975	60	50	2330 ± 132
exp. # 9.2	975	120	50	2387 ± 130
exp. # 3	875	90	42	2331 ± 204
ref.	875	90	33	2266 ± 174
exp. # 5.3	775	60	33	1993 ± 127
exp. # 6.2	775	60	50	1823 ± 97
exp. # 7.2	775	120	50	1932 ± 153
exp. # 8.2	775	120	33	1939 ± 140

Table 5: Hardness results of the coatings.

According to Pareto plot analysis (Figure 30) the process temperature has a significant effect on coating hardness. The process pressure and amount of hydrogen (H_2) have hardly any influence on the hardness. Factorial model (Figure 31) indicates that the coating hardness will increase with increasing process temperature.

© Technion - Israel Institute of Technology, Elyachar Central Library

Term	Orthog Estimate
Temp. [C](775,975)	213.6898
Pressure [mbar]*H2 [L]	53.5874
H2 [L](0,50)	-43.4056
Temp. [C]*Pressure [mbar]	-29.0130
Temp. [C]*Pressure [mbar]*H2 [L]	17.2289
Pressure [mbar](60,120)	-16.6699
Temp. [C]*H2 [L]	1.5317

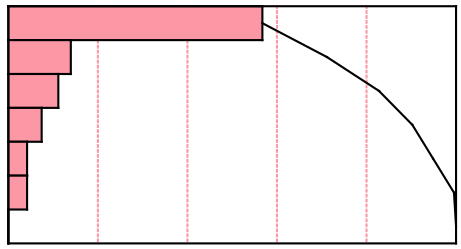

Figure 30: Pareto plot for hardness results.

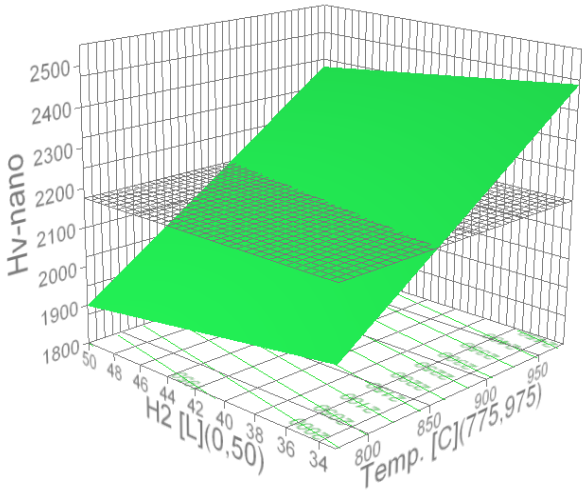

Figure 31: Factorial model for hardness results.

4.3.3 Evaluation of the adhesion

All experimental coatings were tested for adhesion quality. The quality of coating adhesion was determined by indentation. Coating/substrate deformation was achieved by implementing load of 20kgF using a Vickers indenter. All experimental coatings passed this qualitative adhesion test successfully with no coating peeled areas after indentation.

© Technion - Israel Institute of Technology, Elyachar Central Library

4.4 Thermal oxidation

Oxidation rates of 0.9 - 4.5 mm/h were recorded for TiCN MT CVD coatings during heat treatments for 60 minutes in open air furnace at 800 °C (Table 6).

exp #	Temp. [^{0}C]	Pressure [mbar]	H_2 [L]	Oxidation rate T=800^{0}C [µm/h]
exp. # 1.3	975	120	33	1.2 ± 0.1
exp. # 2.2	975	60	33	1.9 ± 0.1
exp. # 4.3	975	60	50	0.9 ± 0.1
exp. # 9.2	975	120	50	1.2 ± 0.1
exp. # 3	875	90	42	3.1 ± 0.1
ref.	875	90	33	3.4 ± 0.1
exp. # 5.3	775	60	33	4.5 ± 0.1
exp. # 6.2	775	60	50	4.5 ± 0.1
exp. # 7.2	775	120	50	4.5 ± 0.1
exp. # 8.2	775	120	33	4.5 ± 0.1

Table 6: Oxidation rate measurements of trial coatings.

It is clear from Pareto plot analysis (Figure 32) that the process temperature has a significant effect on coating oxidation resistance. Other deposition parameters (pressure, H_2) have almost no influence the oxidation rate.

Factorial model (Figure 33) indicates that the oxidation rate will increase with increasing process temperature.

Term	Orthog Estimate
Temp. [C](775,975)	-1.431084
H2 [L](0,50)	-0.150643
Temp. [C]*H2 [L]	-0.111803
Temp. [C]*Pressure [mbar]*H2 [L]	0.111803
Pressure [mbar]*H2 [L]	0.111803
Pressure [mbar](60,120)	-0.044721
Temp. [C]*Pressure [mbar]	-0.044721

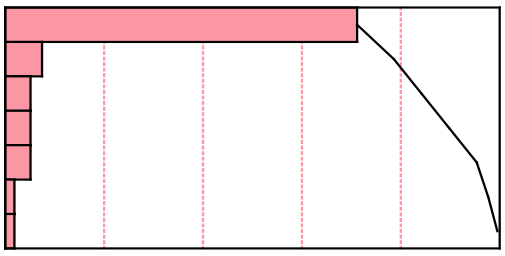

Figure 32: Pareto plot for oxidation rate measurements.

© Technion - Israel Institute of Technology, Elyachar Central Library

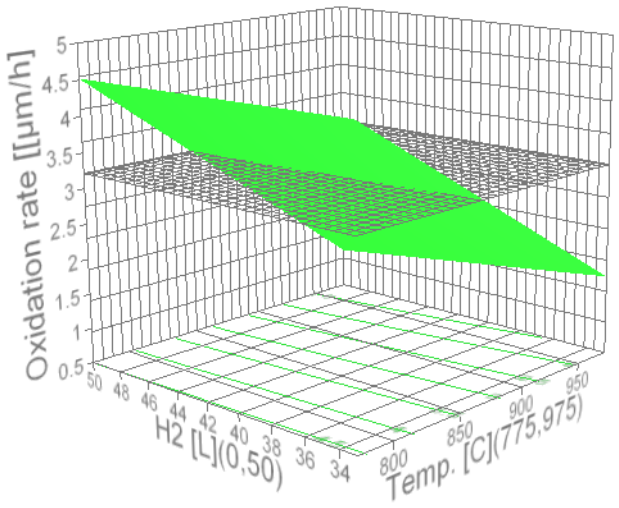

Figure 33: Factorial model of oxidation rate measurements.

We can summarize that a lower oxidation rate can be achieved with increasing coating deposition temperature. This means that high temperature coatings are more resistant to oxidation than low temperature coatings.

4.5 Tribological properties

4.5.1 Interrupted cutting test on SAE1060

Under impact conditions the coatings show totally different behaviors. While high temperature coated inserts are damaged after several minutes, low temperature coatings show an improve performance. The failure of the inserts is caused due to the sudden cutting edge fracture, as presenting Figure 34.

Based on the results, TiCN MT coatings deposited at low temperature (775^{o}C) showed improved cutting performance under interrupted conditions. Cutting test results are presented in Figure 35. These results will be discussed in more detail later.

© Technion - Israel Institute of Technology, Elyachar Central Library

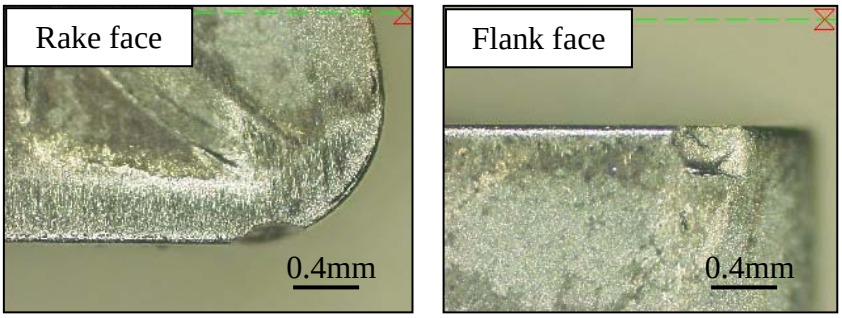

Figure 34: Typical failure during interrupted conditions.

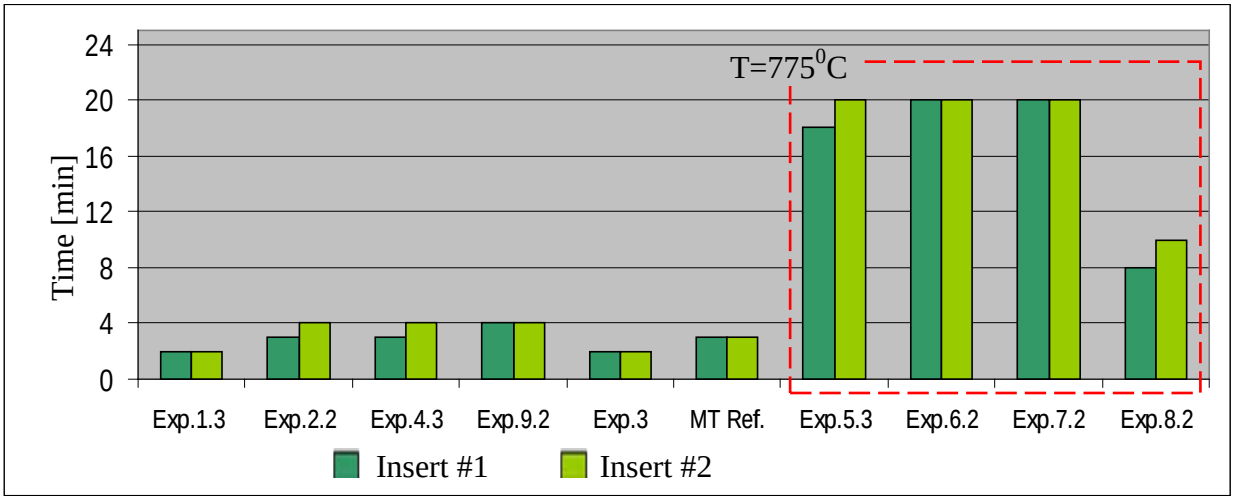

Figure 35: Interrupted cutting test results.

4.5.2 Continuous cutting test on AISI 1045

Figure 36 shows the flank and rake typical wear progress, i.e. the increase in flank and rake wear with cutting time, of the coated inserts during the metal cutting test. All coatings display similar tribological properties, based on the abrasion wear resistance (Figure 37).

© Technion - Israel Institute of Technology, Elyachar Central Library

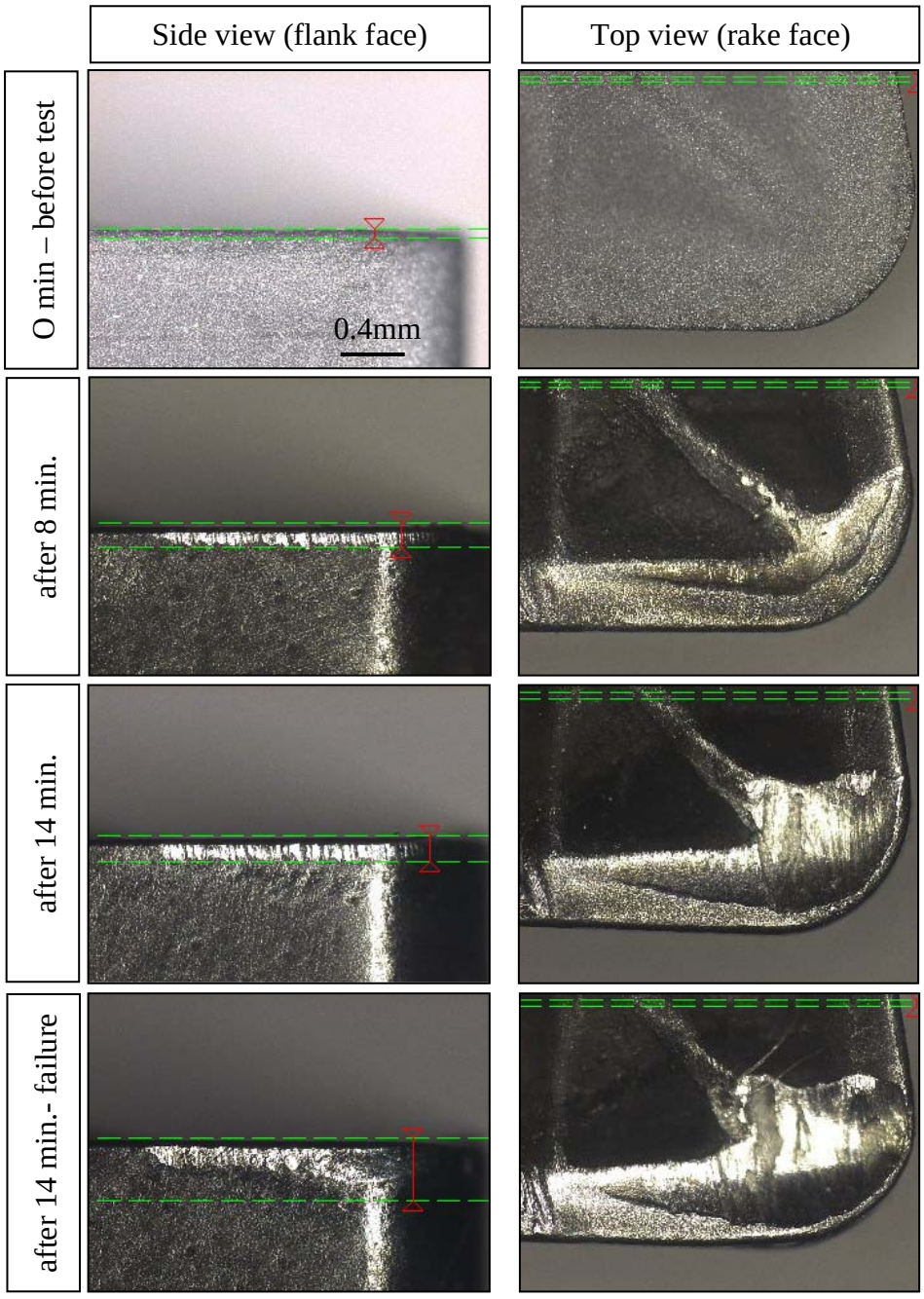

Figure 36: Progress of wear during continuous cutting test (scale-bar is the same for all images).

© Technion - Israel Institute of Technology, Elyachar Central Library

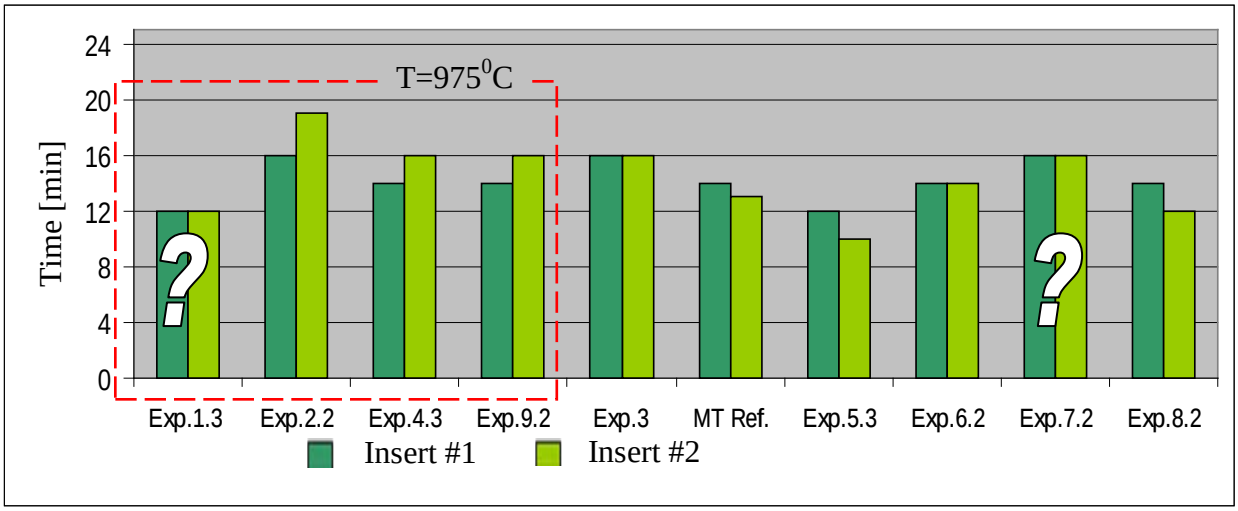

Figure 37: Continuous cutting test results.

No significant difference between coatings performance was found according to these results. However, after correlating the results of coating thickness and machining it is possible to identify some trends.

It was found that high temperate coatings are more wear resistant compared to low temperature coatings. Exp. 1.3 and Exp.7.2 behaves anomalously due to a varying thickness coating. Exp. 1.3 (975°C) with a relatively low coating thickness, 6-10µm. Exp.7.2 (775 °C) with a relatively high coating thickness, 13µm.

© Technion - Israel Institute of Technology, Elyachar Central Library

5 DISCUSSION

5.1 Influence of deposition parameters on MT-TiCN microstructure

It was found that the microstructure of the coatings varied with temperature. A five-fold structure was found in high temperature deposition conditions. Ino explained a pentagonal structure on the basis of a multiple twinning mechanism [43]. He suggested that the pentagonally-shaped grains were composed of five identical tetrahedra with (111) faces. His suggestion is in agreement with our EBSD findings. Also Robinson and Gillet [44] and Yang et al. [45] suggested that decahedral particles are formed with a five-fold orientation. The (111) plane of titanium carbon nitride usually serves as the twin plane [37]. It was found, that the angle between two grains is 70.53° with common (111) planes. This angle is 1.47° smaller than 72° that is required to cover 360° by five grains. The angle of 7.33° must be accommodated by elastic strain. Nassau [46] found that a five-fold twinned crystal is formed also in diamonds. He explained that the crystal has (111) twin planes at re-entrant angles.

Figure 38 is an enlarged view of Figure 18 (high temperature TiCN-MT) where many twin planes can be seen. It shows clearly that some of the twin planes penetrate into two or three fingers of the five-fold twinned crystal. It indicates that the five-fold twinned crystal is a result of growth from the same nucleus. It is not an aggregate of five independent crystals.

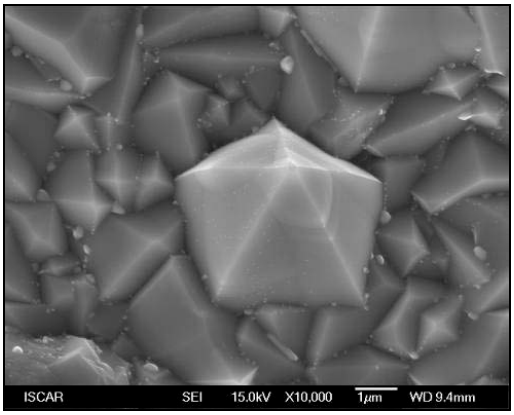

Figure 38: SEM micrograph of the coarse microstructure nucleation within a fine matrix.

© Technion - Israel Institute of Technology, Elyachar Central Library

The five-fold twinned crystals were examined by XRD and EBSD and the [220] growth direction was identified as that of pure TiN. The [111] growth direction of pure TiC was also inspected. It was found by Holzschuh that the C:N ratio increases with decreasing process temperature [23].

It's reasonable to assume that the nucleation of twinned coarse crystals within a fine columnar matrix is caused by the variation of the carbon content which effects the lattice parameter of the TiCN MT coatings. TiCN-MT coatings deposited at high temperature (975^{o}C) do not consist of TiCN grains with a fixed composition. The balance of carbon and nitrogen in the columnar grains can be changed by altering the deposition temperature. In fact, TiCN coatings can be produced with the composition TiC_xN_{1-x}, where x ranges from 0 to 1 and nitrogen can substitute for carbon, which will affect the mechanical properties.

5.2 Influence of MT-TiCN microstructure on mechanical properties

5.2.1 Surface Roughness dependence on microstructure

The growth rate of the five-fold twinned crystals is very large. This could be explained by twin intersection which is a permanent source of steps, thereby providing an easy growth rate mechanism similar to the spiral growth mechanism (see Figure 39) [47].

Growth spirals are formed in crystals containing dislocations with a Burgers vector not parallel to the surface of the crystal (Figure 39). At the intersection point of the dislocation with the surface, a step is formed with a height equal to the component of the Burgers vector that is normal to the surface. During the growth process this step turns around the dislocation line, by laying down a heliocidal atomic plane, which forms a new atomic layer.

© Technion - Israel Institute of Technology, Elyachar Central Library

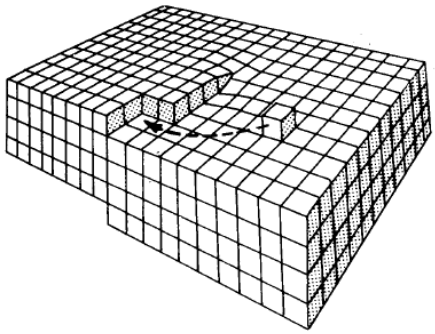

Figure 39: Spiral growth mechanism [47].

5.2.2 Hardness dependence on microstructure

It was found that the fast growth rate of the five-fold microstructure is at the expense of other grains, as presented in Figure 40. According to theoretical considerations, increasing temperature increases the reaction kinetics on the surface [35]. We can postulate that by increasing temperature, the driving force for nucleation is enhanced and consequently the grain size decreased, correlated to a higher hardness.

It was already found that the TiN grain size decreased with increasing temperature, and increasing the deposition temperature can decrease the deposition rate [35].

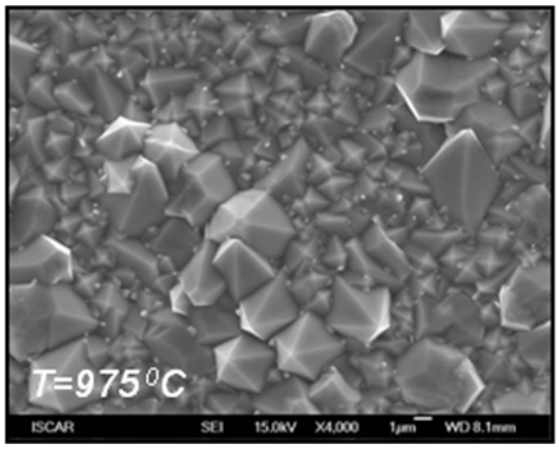

Figure 40: SEM plan-view image of the high temperature coating.

The hardness of the high temperature coatings follows the expected trend according to their grain size distribution, since the hardness is higher with decreasing grain size. This

dependence could be explained by the Hall–Petch relation where hardness is inversely related to the square root of grain diameter [52].

5.2.3 Oxidation resistance

It was already presented that the composition of TiC_xN_{1-x} coatings depends on the deposition temperature. Past works showed that the C:N ratio increases with decreasing of the process temperature [23]. This means that with decreasing process temperature more TiCN grains with lower carbon content will appear. Increasing the process temperature should lead to the appearance of TiCN grains with a higher nitrogen content.

It is known that TiN is more oxidation resistant than TiC [8]. Therefore, the decrease of TiC_xN_{1-x} carbon content should increase oxidation resistance. These facts explain why the high temperature coatings are more stable to oxidation than low temperature coatings.

5.3 Cutting tests

5.3.1 Interrupted cutting test

As interrupted cutting operation goes on, the coating and substrate begins to crack. The coated carbide insert then fails, sudden fracture occurs, and loses cutting ability. Experiments show that the failure mechanism of coated carbide tools is mainly caused by fracture and not due to extend wear development (Figure 34).

It was found that TiCN MT coatings with low temperature deposition (750^{o}C) tend to be more stable in interrupted cutting conditions because of the formation of fine cracks (Figure 27) and low hardness (Figure 31). Figure 41 schematically presents the relation between penetration depth and crack type.

© Technion - Israel Institute of Technology, Elyachar Central Library

© Technion - Israel Institute of Technology, Elyachar Central Library

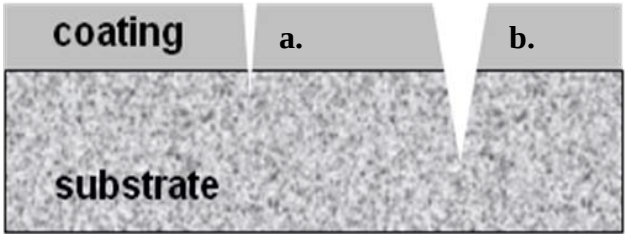

Figure 41: Schematic presentation of cracks penetration depth. (a) fine crack after deposition at low temperature; (b) wide crack after deposition at high temperature.

Coatings often suffer from thermal cracking resulting differences in the thermal expansion coefficient of the coating and the substrate. The thermal expansion coefficient for WC-Co is 5.4×10^{-6}, and 8.4×10^{-6} for TiCN [48-51].

It was concluded that the fine cracks (Figure 41a) formed in coatings deposited at low temperature are due to stress relaxation. Wide cracks (Figure 41b) formed in coatings deposited at higher temperatures are a result of the larger tensile residual stress in the coating due to the total temperature difference from the deposition temperature to room temperature. These results are in agreement with Matsue's [53] findings. Matsue found that thermal residual stresses in coatings depends on the annealing process and was determined from:

$$\sigma_{th} = \frac{E_{film}}{1 - \nu_{film}} \left(\alpha_{film} - \alpha_{substrate} \right) \Delta T \qquad (6)$$

where: σ_{th} is the thermal residual stress, E_{film} is Young's modulus of coating, ν_{film} is Poisson's ratio of the coating, σ_{film} is the thermal expansion coefficient of the coating, $\sigma_{substrate}$ is the thermal expansion coefficient of the substrate, and ΔT is a difference between deposition temperature and room temperature.

For the case of low deposition temperatures, ΔT is small, and fine cracks are formed due to the limited tensile residual stress. However, for the case of high deposition temperatures, ΔT is larger, and wide cracks are formed due to high tensile residual stress.

© Technion - Israel Institute of Technology, Elyachar Central Library

Wide cracks lead to reduction in tool life attributable to deeper penetration into the substrate.

5.3.2 Continuous cutting test results dependence mechanical properties

During continues cutting tests two normally flat surfaces are pressed together, and contacts form at discrete point. The true contact area under normal load is thus only a fraction of the total or nominal surface area. Deformation occurring at contact points can be elastic, plastic, or mixed elastic-plastic, depending on the surface roughness and coating hardness.

It was found that coating roughness and hardness depends on process temperature (Figure 29 and Figure 31 respectively). Surface roughness of a slightly higher order may increase friction and wear, promote noise, or cause rough running and premature failure of the insert.

In the case of abrasive wear, the hardness of the coating is dominant. According to the machining results (Figure 37) high temperature TiCN MT coatings give higher wear resistance compared to low temperature coatings. This goes parallel with the higher hardness and high chemical stability of high temperature coatings, as presented in Figure 31 and Figure 33. The higher hardness was achieved due to the small grain size and good oxidation resistance due to low carbon content.

© Technion - Israel Institute of Technology, Elyachar Central Library

6 SUMMARY AND CONCLUSIONS

The influence of CVD deposition variables such as temperature (T), H_2 and pressure on the microstructure, surface morphology, mechanical properties, thermal stability and tribological properties of TiCN MT coatings on tungsten carbide substrates was investigated.

We examined the texture and grain size of coatings deposited by CVD using XRD and EBSD. The relation between microstructure and mechanical properties, such as hardness and roughness, was determined. It was found that deposition temperature is a critical factor that can be effectively used to control the microstructure of the coating. Control of the microstructure is imperative to optimize its mechanical properties.

High temperature deposition conditions result in the formation of (220) oriented films. Low temperature deposition conditions result in the formation of (311) and (422) oriented films. The influence of the process parameters on interrupted cutting was investigated. TiCN-MT coatings deposited at low temperature (775^{o}C) tend to be more stable in interrupted cutting conditions because of closed surface cracks and lower hardness. TiCN-MT coatings deposited at high temperature (975^{o}C) showed better results in continuous cutting because of a lower oxidation rate and high hardness.

© Technion - Israel Institute of Technology, Elyachar Central Library

7 RECOMMENDATION FOR FUTURE WORK

Modern coating technology enable multilayered coatings in order to handle the higher temperature required for high speed cutting conditions. Various combinations of multiple coatings should be developed, and must also combine the best properties from coating materials. Preferred TiCN-MT coating with combination of alumina (Al_2O_3) should be established to provide inserts with broad applications ranges. Oxidation resistance and ability to maintain hot hardness of alumina coating can significantly improve cutting performance.

© Technion - Israel Institute of Technology, Elyachar Central Library

8 REFERENCES

[1] Boothroyd G., Fundamentals of metal machining and machine tools, McGraw Hill, Tokyo (1981).

[2] Kalass W., Grey C, Reiter A., Endrino J.L. and Derflinger V., Modem coatings in high performance cutting applications, Proceedings of 16th. Int. Plansee Seminar, 30 May - 3 June, Reutte, Austria, (2005) 800-811.

[3] AB Sandvik Coromant, Modem metal cutting, A practical handbook, Sweden (1994).

[4] Exner H.E., Qualitative and quantitative interpretation of toughness testing of microstructures in cemented carbides, Science of Hard Materials, Plenum Press, New York, (1983) 233-262.

[5] Carpenter M., Transverse rupture testing of fine grain size hardmetals - parameters influencing the results, Presented at the Powder Metallurgy Association of South Africa, July (1998).

[6] Schaller R., Mari D., Maamouri M. and Ammann J.J., Mechanical behavior of WC - 11 wt.% Co studied by bending tests, internal friction and electron microscopy, Journal of Hard Materials, 3, (1992) 351-362.

[7] Shaviv R., Synthesis of TiN and TiN_xC_y: Optimization of reaction parameters, Materials Science and Engineering, A209, (1996) 345-352.

[8] Igarashi T, Kobayashi M. and Takatsu S., Effects of TiN on microstructure and properties of WC-based cemented carbides, Inst. Phys. Conf. Ser. No. 75: Chapter 6, Paper presented at 2nd Int. Conf. Science Hard Mater., Rhodes, (1984) 337-348.

[9] M. Fallqvist, M. Olsson, S. Ruppi, Abrasive wear of multilayer [kappa]-Al2O3-Ti(C,N) CVD coatings on cemented carbide, Wear 263 (2007) 74-80.

[10] S. Soderberg, M. Sjostrand, B. Ljungberg, Advances in coating technology for metal cutting tools, Metal Powder Report 56 (2001) 24-30.

[11] M.T. Laugier, Adhesion at elevated temperatures of TiN coatings on cemented carbides, Materials Science and Engineering: A 105-106 (1988) 513-516.

© Technion - Israel Institute of Technology, Elyachar Central Library

[12] Brookes KJA. World directory and handbook of hard metals Int Carb Data, East Barnet, Herts EN4 8DN, GB (1982).

[13] H.E. Evans, Cracking and spalling of protective oxide layers, Materials Science and Engineering: A 120-121 (1989) 139-146.

[14] K. Hokkirigawa, K. Kato, Z.Z. Li, The effect of hardness on the transition of the abrasive wear mechanism of steels, Wear 123 (1988) 241-251.

[15] P.R. Chalker, S.J. Bull, D.S. Rickerby, A review of the methods for the evaluation of coating-substrate adhesion, Materials Science and Engineering: A 140 (1991) 583-592.

[16] P.C. Jindal, D.T. Quinto, G.J. Wolfe, Adhesion measurements of chemically vapor deposited and physically vapor deposited hard coatings on WC-Co substrates, Thin Solid Films 154 (1987) 361-375.

[17] H.-W. Chen, V. Rudolph, The 3-D structure of polycrystalline diamond film by electron backscattering diffraction (EBSD), Diamond and Related Materials 12 (2003) 1633-1639.

[18] S. Kudapa, K. Narasimhan, P. Boppana, W.C. Russell, Characterization and properties of MTCVD TiCN and MTCVD ZrCN coatings, Surface and Coatings Technology 120-121 (1999) 259-264.

[19] Randle, V.; Engler, O., Introduction to Texture Analysis, Gordon and Breach Science (2000).

[20] Schwartz, A. J.; Kumar, M.; Adams, B. L., Electron Backscatter Diffraction in Materials Science, Plenum Publishing Corporation (2000).

[21] S. Soderberg, M. Sjostrand, B. Ljungberg, Advances in coating technology for metal cutting tools, Metal Powder Report 56 (2001) 24-30.

[22] M.H. Staia, D.G. Bhat, E.S. Puchi-Cabrera, J. Bost, Characterization of chemical vapor deposited HfN multilayer coatings on cemented carbide cutting tools, Wear 261 (2006) 540-548.

[23] H. Holzschuh, Chemical-vapor deposition of wear resistant hard coatings in the Ti-B-C-N system: properties and metal-cutting tests, International Journal of Refractory Metals and Hard Materials 20 (2002) 143-149.

© Technion - Israel Institute of Technology, Elyachar Central Library

[24] K. Holmberg, A. Matthews, H. Ronkainen, Coatings tribology--contact mechanisms and surface design, Tribology International 31 (1998) 107-120.

[25] H. Ollendorf, D. Schneider, A comparative study of adhesion test methods for hard coatings, Surface and Coatings Technology 113 (1999) 86-102.

[26] H.E. Evans, Cracking and spalling of protective oxide layers, Materials Science and Engineering: A 120-121 (1989) 139-146.

[27] T. Sugama, CVD-titanium carbonitride coatings as corrosion-preventing barriers for steel in acid-brine steam at 200°C, Materials Letters 38 (1999) 227-234.

[28] S. Ruppi, Deposition, microstructure and properties of texture-controlled CVD [alpha]-Al2O3 coatings, International Journal of Refractory Metals and Hard Materials 23 (2005) 306-316.

[29] S. Ruppi, A. Larsson, Deposition, microstructure, and properties of nanocrystalline Ti(C,O,N) coatings, Journal of Vacuum Science & Technology A: Vacuum, Surfaces, and Films 21 (2003) 66-75.

[30] K. Narasimhan, S.P. Boppana, D.G. Bhat, Development of a graded TiCN coating for cemented carbide cutting tools--a design approach, Wear 188 (1995) 123-129.

[31] P.G. Seminar, J. Kiviö, Hard coatings of cutting tools

[32] C.V. Thompson, R. Carel, J., Mechanics and Physics of Layered and Graded Materials, Journal of the Mechanics and Physics of Solids (1996) 657-673.

[33] A. Forn, J.A. Picas, G.G. Fuentes, E. Elizalde, Mechanical and tribological properties of TiCxN1-x wear resistant coatings, International Journal of Refractory Metals and Hard Materials 19 (2001) 507-513.

[34] J. Ding, Y. Meng, S. Wen, Mechanical properties and fracture toughness of multilayer hard coatings using nanoindentation, Thin Solid Films 371 (2000) 178-182.

[35] H. Kashani, M. Heydarzadeh Sohi, H. Kaypour, Microstructural and physical properties of titanium nitride coatings produced by CVD process, Materials Science and Engineering A 286 (2000) 324-330.

© Technion - Israel Institute of Technology, Elyachar Central Library

[36] A. Larsson, M. Halvarsson, S. Ruppi, Microstructural changes in CVD [kappa]-Al_2O_3 coated cutting tools during turning operations, Surface and Coatings Technology 111 (1999) 191-198.

[37] A. Larsson, S. Ruppi, Microstructure and properties of Ti(C,N) coatings produced by moderate temperature chemical vapour deposition, Thin Solid Films 402 (2002) 203-210.

[38] S. Park, S.G. Kapoor, R.E. DeVor, Microstructure-Level Model for the Prediction of Tool Failure in Coated WC-Co Cutting Tool Materials During Intermittent Cutting, Journal of Manufacturing Science and Engineering 129 (2007) 893-901.

[39] B. Navinsek, P. Panjan, Oxidation resistance of PVD Cr, Cr-N and Cr-N-O hard coatings, Surface and Coatings Technology 59 (1993) 244-248.

[40] S.J. Bull, D.G. Bhat, M.H. Staia, Properties and performance of commercial TiCN coatings. Part 1: coating architecture and hardness modelling, Surface and Coatings Technology 163-164 (2003) 499-506.

[41] L. Zhou, J. Ni, Q. He, Study on failure mechanism of the coated carbide tool, International Journal of Refractory Metals and Hard Materials 25 (2007) 1-5

[42] S. Goulart-Santos, C. Godoy, M.M.R. Castro, Topographical analysis by 3-D profilometry in the study of the oxidation of Cr-N coated hard metal tools, International Journal of Refractory Metals and Hard Materials 26 (2008) 555-562

[43] S. Ino, J. Phys. Soc. Japan 21 (1966) 346.

[44] F. Robinson and M. Gillet, Thin Solid Films 98 (1982)179.

[45] C.Y. Yang, M.J. Yacaman and K. Heinemann, J. Crystal Growth 47 (1979) 283

[46] K. Nassau, J. Crystal Growth 46 (1979) 165.

[47] D.A. Porter and K.E. Easterling, Phase Transformation in Metals and Alloys (1981) 202.

[48] M.F. Doerner and W.D. Nix, Stresses and Deformation Processes in Thin Films on Substrates, CRC Critical Review Solid State Materials Science14 (1988) 225.

[49] P. Dhaudari, Grain Growth and Stress Relief in Thin Films, Journal of Vacuum Science and Technology 9 (1972) 520.

© Technion - Israel Institute of Technology, Elyachar Central Library

[50] R.W. Hoffman, The Mechanical Properties of Thin Condensed Films, Physics of Thin Films, G. Hass and R.E. Thurn, eds., Academic Press, New York 34 (1966) 211.

[51] F.M. D'Heurle and J.M.E. Harper, Note on the Origin of Intrinsic Stresses in Films Deposited Via Evaporation and Sputtering, Thin Solid Films 171 (1989) 81

[52] Philip C. Yashar and William D. Sproul , Nanometer scale multilayered hard coatings, 55 (1999) 179-190.

[53] T.Matsue, T.Hanabusa and Y.Ikeuchi, X-ray Stress Measurement of Cu/TiN Films, The Society of Materials Science, Japan, 51 (2002) 743-748.

© Technion - Israel Institute of Technology, Elyachar Central Library

מיקרומבנה ותכונות של ציפויי TiCN מסוג CVD

גדי גרינמן

© Technion - Israel Institute of Technology, Elyachar Central Library

מיקרומבנה ותכונות של
ציפויי TiCN מסוג CVD

חיבור על מחקר לשם מילוי חלקי של הדרישות לקבלת התואר
מגיסטר למדעים בהנדסת חומרים

גדי גרינמן

הוגש לסנט הטכניון – מכון טכנולוגי לישראל

אייר תשע"א חיפה מאי 2011

מחקר זה נעשה בהנחיית פרופ' וויין קפלן מהפקולטה להנדסת חומרים בטכניון – מכון טכנולוגי לישראל.

תודות

ברצוני להודות לפרופ' וויין קפלן על ההנחיה והעזרה שנתן לי במשך תקופת המחקר.

הנני מודה לדר' אלכס ברנר, מהמחלקה להנדסת חומרים שבטכניון, על עזרה בביצוע בדיקות SEM-EBSD. תודה נתונה לגב' מריאנה לדרמן על בדיקות XRD ולמר' שגיב קלעי על בדיקות ננו-קושי, קולגות שלי מחברת ישקר .

הכרת תודה מיוחדת לכל בני משפחתי ובעיקר לאשתי אירין, על הסבלנות, תמיכה, אהבה ועזרה רבה לכל אורך תקופת המחקר.

© Technion - Israel Institute of Technology, Elyachar Central Library

© Technion - Israel Institute of Technology, Elyachar Central Library

תקציר

לאורך השנים הבעיה העיקרית בייצור מתק"ש הייתה עמידות לבלאי בקוי חריטה. החריטה היא פעולה שיבוב המתבצעת באמצעות מחרטה כשהכלי הוא בעל חוד (insert) בודד. חוד, או שימה, מוגדרת גיואמטרית נמצא במגע מתמיד עם העובד. העובד מקבל תנוע סיבובית בעוד שהכלי מבצע תנועת קידמה קווית.

הפתרון להתפתחות בלאי היה פשרה של ייצור מתק"ש עם תוספות של TiC , TaC ו- NbC המשפרים עמידות תרמית. השינוי הדרמטי ביותר, ובאותה מידה הפיתוח החשוב ביותר בתעשיית המתק"ש החל עם כניסתן של טכנולוגיות ציפוי חדשות. ע"י המעבר משימה (insert) לא מצופה לשימה מצופה, מהירות החיתוך ואורך חיי השימה עלו בצורה דרסטית.

ישנן שתי שיטות ציפוי עיקריות למתק"ש:

1. CVD(Chemical Vapor Deposition)
2. PVD (Physical Vapor Deposition)

כאשר רוב השימות לאפליקציות חריטה מצופות בתהליך CVD .

בכדי לאפשר שיבוב של חומרים שונים על כלי העיבוד, שימות, להיות בעלי התכונות הבאות:

א. לשמור על קשיות השימות בכל טמפרטורות העבודה.
קשיות השימה חייבת להיות יותר גבוהה מקשיות החומר אותו מעבדים בכל תנאי השיבוב. במידה וקשיות השימה אינה מספקת תתכן כפיפת הפינה החותכת.

ב. התנגדות לבלאי בשחיקה.
חומר כלי השיבוב חייב לגלות התנגדות לבלאי אברזיבי. גודל הבלאי באזורים השונים על השימה קובע את אורך חיי הפינה העובדת.

ג. אדהזיה טובה בין בסיס לציפוי.
אדהזיה לא טובה של הציפוי יכולה לגרום לירידה משמעותית באורך חיי השימה ולפגוע באיכות פני שטח של העובד.

ד. הבדלים קטנים בהתפשטות תרמית בין ציפוי לבסיס.
התאמה טובה בין תכונות הבסיס והציפוי יכולה לצמצם משמעותית הופעת סדקים.

שימות מצופות מאפשרות להגדיל את מהירות השיבוב בהשוואה לכלי עשוי מאותו חומר בכ - 50% או לחלופין אם נשארים באותה מהירות שיבוב אז אורך חיים יכול לגדול בכ- 100%.

הצורות בהן מתגלה בלאי שימות מגוונות ושונות, וכן גם הסיבות לבלאי זה. אולם התהליך הגורם לבלאי הכלי מורכב מאחד או יותר ממנגנוני הבלאי המתרחשים בעת השיבוב.

<u>בלאי אברזיבי</u>

זהו מנגנון שחיקה המתרחש עקב כך שהחלק המתכתי אינו בעל מבנה מטאלורגי הומוגני ומכיל חלקיקים ואזורים קשים. הללו חורשים ופוגעים בשימות למרות קשיותו הגבוהה. גורמים נוספים העוזרים לשחיקה הם תנודות במכונה, טיב פני שטח גרוע (הן של השימות והן של העובד) וכן קיום תחמוצות על פני שטח העובד כתוצאה מתהליך מוקדם כגון חשול או יציקה. במהירות עבוד גבוהה, כלי השיבוב מתחמם מאוד ואז אפקט אברזיה נכר מאוד.

<u>אדהזיה (הדבקה)</u>

עקב המגע, הרצוף והנקי מתחמוצות, בין העובד והשבב לבין כלי החיתוך, נוצרים אזורי ריתוך רגעיים (בטמפרטורה ובלחץ השיבוב) בין השימה, העובד והשבב. ריתוכים אלה נגזרים באזור השבב, בדרך כלל, אך לפעמים נגזרים הם גם באזור הכלי והדבר גורם להתנתקות חומר מן השימות.

<u>חמצון</u>

בפעילות השיבוב מושקעת אנרגיה מכאנית. אנרגיה זו מנוצלת לצורך הפרדת השבב. תהליך זה כרוך במספר פעולות המתרחשות בעת ובעונה אחת :

א. פעולת גזירה (מתרחשת במישור הגזירה).

ב. דיפורמציה של השבב.

ג. חיכוך של השבב והעובד נגד הכלי (באזורי המגע).

האנרגיה המכאנית המושקעת בפעולות הנ"ל הופכת רובה ככולה לחום. החום המתפתח בין העובד והכלי בעת השיבוב הינו אחד הגורמים ההרסניים ביותר המשפעים על אורך החיים של כלי השיבוב. עם עליית טמפרטורת כלי החיתוך יורדת קשיותו, תהליך הבלאי הולך וגובר והוא מאבד את סגולותיו כחומר חותך.

© Technion - Israel Institute of Technology, Elyachar Central Library

תהליך השיבוב, בו מתפתחות טמפרטורות גבוהות נוח לאטומי חמצן שבאוויר להתרכב עם השכבה החיצונית (ציפוי) של שימות החיתוך ולחמצנה. ככל שטמפרטורת השיבוב גבוהה יותר כן יהיה תהליך החמצון מהיר והרסני יותר.

<u>תופעות בלאי אופיניות</u>

בעת השיבוב מתגלות תופעות הבלאי האופיניות הבאות –

א. בלאי פאת השיחרור.
ב. בלאי משטח השיבוב (מכתש).
ג. שברים וסדקים בחומר החיתוך.
ד. דפורמציה פלסטית של השימות.

בלאי של השימות מתפתח בעיקר בשני מקומות :

1. בלאי בפאת השחרור (Flank wear).

בלאי בפאת השחרור יכול לנבוע כתוצאת אדהזיה לא תקינה או שחיקה מוגברת של הציפוי.

2. בלאי מכתש (Crater Wear).

בלאי מכתש, בחלק העליון של השימה, יכול לנבוע בגלל התחמצנות ופירוק הציפוי, פירוק שכבה מגנה. תהליך זה קורה עקב הטמפרטורה הגבוהה שנוצרת בזמן השיבוב ($1000^{o}C$).

ציפויי טיטניום קרבון ניטריד (MTTiCN) בטמפרטורות בינוניות ידועים באמידותן בפני שחיקה. לציפויים אלו יש שימוש נרחב בעיבוד שבבי של ברזל יציקה אפור, ברזל יציקה נודולרי ,פלדות. עיבוד שבבי של מתכות דורש יציבות פינה חותכת מבחינת חוזק ועמידות בפני שחיכה. MTTiCN הינו ציפוי הנפוץ ביותר בישום של כלים לעיבוד שבבי.

בעבודה זו בוצעו ניסיונות לשקע TiCN בתנאי שיקוע שונים. נחקרו השפעות של טמפרטורת שיקוע, לחץ וספקות מימן על כיווניות מעודפת , גודל גרעין, פני שטח, קצב שיקוע, קושי ועמידות תרמית. כיווניות מועדפת של MT TiCN אופיין על ידי דיפרקציית קרני X (XRD). שימוש במיקרוסקופ אלקטרונים סורק (SEM) ומיקרוסקופ אופטי נעשה לאפיון מורפולוגיית פני שטח.

© Technion - Israel Institute of Technology, Elyachar Central Library

ציפויי TiCN MT בעלי מיקרומבנה של עמודות עם כיווניות מועדפת התלוי בפרמטרי שיקוע. תוצאות הגדירו את טמפרטורת שיקוע כפרמטר החשוב ביותר לשליטה יעילה במיקרומבנה ו- מורפולוגיית פני הציפוי.

תהליכי ציפוי בטמפרטורה גבוהה מאפשרות גידול שכבות באוריינטציה מועדפת של {220}. מצד שני, בטמפרטורות נמוכות ניתן לקבל אוריינטציות של {311} ו- {422}
שליטה במיקרומיבנה של ציפויים מאפשרת קביעת תכונות מכאניות הדרושות באפליקציות שיבוב מסוימות. לדוגמא, ציפויי TiCN MT בטמפרטורה של $750^{o}C$ מציגים תוצאות טובות בעיבוד פלדות בתנאי שיבוב לא יציבים , וזאת בגלל קושי הנמוך של הציפויים הללו. כנגד, ציפויי TiCN MT בטמפרטורה גבוהה ($950^{o}C$) מציגים תוצאות טובות יותר בעיבוד פלדות בתנאי שיבוב יציבים , וזאת בגלל קושי הגבוה ועמידות תרמית טובה.

© Technion - Israel Institute of Technology, Elyachar Central Library